Physiological and climate controls on foliar mercury uptake by European tree species

Lena Wohlgemuth[1], Pasi Rautio[2], Bernd Ahrends[3], Alexander Russ[4], Lars Vesterdal[5], Peter Waldner[6], Volkmar Timmermann[7], Nadine Eickenscheidt[8], Alfred Fürst[9], Martin Greve[10], Peter Roskams[11], Anne Thimonier[6], Manuel Nicolas[12], Anna Kowalska[13], Morten Ingerslev[5], Päivi Merilä[14], Sue Benham[15], Carmen Iacoban[16], Günter Hoch[1], Christine Alewell[1], Martin Jiskra[1]

[1] Department of Environmental Sciences, University of Basel, Basel, CH-4056, Switzerland
[2] Natural Resources Institute Finland (Luke), Ounasjoentie 6, 96200 FI-Rovaniemi, Finland
[3] Department of Environmental Control, Northwest German Forest Research Institute (NW-FVA), Grätzelstr. 2, D-37079 Göttingen, Germany
[4] Landesbetrieb Forst Brandenburg, Alfred-Möller-Straße 1, D-16225 Eberswalde, Germany
[5] Department of Geosciences and Natural Resource Management, University of Copenhagen, Rolighedsvej 23, DK-1958 Frederiksberg C, Denmark
[6] Swiss Federal Institute for Forest, Snow and Landscape Research (WSL), Zürcherstrasse 111, CH-8903 Birmensdorf, Switzerland
[7] Norwegian Institute of Bioeconomy Research (NIBIO), NO-1431 Ås, Norway
[8] State Agency for Nature, Environment and Consumer Protection of North Rhine-Westphalia (LANUV), Leibnizstr. 10, D-45659 Recklinghausen, Germany
[9] Department of Forest Protection, Austrian Federal Research Centre for Forests, Vienna, A-1130, Austria
[10] Research Institute for Forest Ecology and Forestry Rhineland-Palatinate (FAWF), Hauptstr. 16, D-67705 Trippstadt, Germany
[11] Research Institute for Nature and Forest (INBO), Gaverstraat 4, B-9500 Geraardsbergen, Belgium
[12] Office National des Forêts (ONF), Département Recherche-Développement-Innovation, F-77300 Fontainebleau, France
[13] Forest Research Institute, Sekocin Stary, Braci Lesnej 3, PL-05-090 Raszyn, Poland
[14] Natural Resources Institute Finland (Luke), Paavo Havaksentie 3, FI-90570 Oulu, Finland
[15] Forest Research, Alice Holt Lodge, Farnham Surrey, GU51 3QE, United Kingdom
[16] Department of Ecology, "Marin Dracea" National Institute for Research and Development in Forestry, Campulung Moldovenesc Station, 73 bis Calea Bucovinei, RO-725100 Campulung Moldovenesc, Romania

Correspondence to: Lena Wohlgemuth (lena.wohlgemuth@unibas.ch), Martin Jiskra (martin.jiskra@unibas.ch)

Abstract.

Despite the importance of vegetation uptake of atmospheric gaseous elemental mercury (Hg(0)) within the global Hg cycle, little knowledge exists on the physiological, climatic and geographic factors controlling stomatal uptake of atmospheric Hg(0) by tree foliage. We investigate controls on foliar stomatal Hg(0) uptake by combining Hg measurements of 3,569 foliage samples across Europe with data on tree species traits and environmental conditions. To account for foliar Hg accumulation over time, we normalized foliar Hg concentration over the foliar life period from the simulated start of the growing season to sample harvest.

The most relevant parameter impacting daily foliar stomatal Hg uptake was tree functional group (deciduous versus coniferous trees). On average, we measured 3.2 times higher daily foliar stomatal Hg uptake rates in deciduous leaves than in coniferous needles of the same age. Across tree species, for foliage of beech and fir, and at two out of three forest plots with more than 20 samples, we found a significant ($p < 0.001$) increase in foliar Hg values with respective leaf nitrogen concentrations. We therefore suggest, that foliar stomatal Hg uptake is controlled by tree functional traits with uptake rates increasing from low to high nutrient content representing low to high physiological activity. For pine and spruce needles, we detected a significant linear decrease of daily foliar stomatal Hg uptake with the proportion of time during which water vapor pressure deficit (VPD) exceeded the species-specific threshold values of 1.2 kPa and 3 kPa, respectively. The proportion of time within the growing season during which surface soil water content (ERA5-Land) in the region of forest plots was low correlated negatively with foliar Hg uptake rates of beech and pine. These findings suggest that stomatal uptake of atmospheric Hg(0) is inhibited under high VPD conditions and/or low soil water content due to the regulation of stomatal conductance to reduce water loss under dry conditions. Other parameters associated with forest sampling sites (latitude and altitude), sampled trees (average age and diameter at breast height) or regional satellite observation-based transpiration product (GLEAM) did not significantly correlate with daily foliar Hg uptake rates. We conclude that tree physiological activity and stomatal response to VPD and soil water content should be implemented in a stomatal Hg model, to assess future Hg cycling under different anthropogenic emission scenarios and global warming.

1 Introduction

Mercury (Hg) is a toxic pollutant that is emitted by anthropogenic and geogenic activities into the atmosphere, where it can be transported over large distances and is eventually transferred to terrestrial and ocean surfaces by dry or wet deposition (Bishop et al., 2020). From a public health perspective, transfer rates of Hg to aquatic ecosystems are particularly relevant within this cycle, since Hg bioaccumulation in fish for consumption represents the most important Hg exposure pathway to many communities internationally (UN Environment, 2019). In order to constrain future Hg levels in edible fish and to assess how Hg exposure responds to curbed anthropogenic Hg emissions under the policies implemented by the 2017 UN Minamata convention on mercury, it is essential to understand and quantify all major net deposition fluxes within the global Hg cycle.

Wet deposition occurs when water-soluble oxidized Hg(II) is washed out from the atmosphere with rainwater (Driscoll et al., 2013; Sprovieri et al., 2017) or by cloud water interception (Weiss-Penzias et al., 2012). In a dry deposition process, gaseous elemental Hg(0) and Hg(II) directly bind to surfaces (Bishop et al., 2020) or Hg(0) is taken up by plants (Zhou et al., 2021). For more than two decades, vegetation has been recognized as important vector for Hg(0) dry deposition within the terrestrial Hg cycle (Rea et al., 1996, 2002; Grigal, 2003). Based on this seminal work, researchers have since highlighted that vegetation impacts Hg levels of all other environmental compartments within the active Hg cycle (AMAP and UNEP, 2019; Bishop et al., 2020; Zhou et al., 2021). Vegetation uptake of Hg(0) governs the seasonality of atmospheric Hg(0) in the Northern Hemisphere with concentration minima in summer at the end of the growing season (Jiskra et al., 2018). Thus, vegetation has been suggested to operate like a global Hg pump (Obrist, 2007; Jiskra et al., 2018). Atmospheric Hg(0) taken up by vegetation is oxidized to Hg(II) within the plant tissue (Manceau et al., 2018) and transferred to soils via litterfall (Iverfeldt, 1991; Schwesig and Matzner, 2000; Rea et al., 2001; Graydon et al., 2008; Risch et al., 2012; Jiskra et al., 2015; Wright et al., 2016; Wang et al., 2016; Risch et al., 2017). Moreover, in forests, Hg deposition to the ground may occur by wash-off of Hg(0) from plant surfaces via throughfall and by Hg(0) uptake into woody tissues, lichen, mosses and soil litter (Wang et al., 2020; Obrist et al., 2021). Mercury sequestered by forest ecosystems accumulates in soil and may subsequently be transported from watersheds to streams, rivers and the ocean, where it can bioaccumulate in fish (Drenner et al., 2013; Jiskra et al., 2017; Sonke et al., 2018).

Concerning the mechanism of Hg accumulation in foliage, there are multiple lines of evidence that leaf stomata control the foliar Hg(0) uptake flux to terrestrial ecosystems: (i) Hg concentrations were found to be higher in internal foliar tissues than on leaf surfaces (Laacouri et al., 2013); (ii) experiments revealed that isotopic Hg tracers are transferred from the air to the leaf interior (Rutter et al., 2011); (iii) foliar Hg concentrations are associated with leaf stomatal density and net photosynthesis (Laacouri et al., 2013; Teixeira et al., 2018); (iv) the isotopic composition of foliage is discriminated in heavy isotopes compared to atmospheric Hg(0) (Demers et al., 2013; Enrico et al., 2016; Yu et al., 2016; Jiskra et al., 2019); (v) temporal and vertical variations of net foliar Hg(0) uptake fluxes in trees agree with the mechanism of stomatal Hg(0) uptake (Wohlgemuth et al., 2020). While there is increasing consensus that vegetation uptake of atmospheric Hg(0) occurs via the stomatal pathway, there remain research gaps regarding parameters regulating this stomatal Hg(0) uptake (Zhou et al., 2021). Consequently, the Hg(0) dry deposition flux to terrestrial surfaces in Hg Earth System Models is generally parametrized by static inferential or resistance-in-series approaches (Travnikov et al., 2017). Ecosystem processes, including canopy gas exchange, are sensitive to climate conditions (Running and Coughlan, 1988) and vary between different plant species (Reich et al., 2003). Trees control leaf diffusive gas fluxes through their stomata in order to optimize the diffusive influx of carbon dioxide for photosynthesis, while averting excessive loss of water vapor to the atmosphere (Körner, 2013). The regulation of stomata allows trees to dynamically adjust their metabolism to climatic conditions (temperature, atmospheric humidity, water vapor pressure deficit, solar radiation) and site-specific limitations (soil moisture, nutrient availability) under the constraints of tree-specific prerequisites (leaf structure, leaf life span, water use efficiency).

In this study we aim to improve the process understanding of the stomatal Hg(0) uptake with the long-term goal to advance the parameterization of the foliar Hg(0) uptake in Hg Earth System Models. The objectives of the study were: (i) to investigate how foliar Hg(0) uptake depends on the physiological traits of tree species, and (ii) to study how stomatal response of trees to climate conditions control foliar Hg(0) uptake. We address these objectives by analyzing a large dataset of foliar Hg uptake rates, tree functional traits and climate conditions across natural gradients in European forests covering various tree species and climate conditions.

2 Material and Methods

2.1 Foliage sampling and data set description

The final dataset for this study comprises Hg concentrations of 3,569 foliage samples from 2015 and 2017, of which 2,129 samples were provided by 17 participating countries of the UNECE International Co-operative Programme on Assessment and Monitoring of Air Pollution Effects on Forests (ICP Forests). The samples include sun exposed leaves and needles from the upper third of the tree canopy of 5 trees (Austrian Bio-Indicator Grid: 2 trees) of the main species on the plot taken during full development in summer (deciduous species) or at the onset of dormant season in autumn (evergreen species) using harmonized national methods according to the ICP Forests Manual (Rautio et al. 2016) as described e.g. in Jonard et al. (2015). Around 10% of samples were taken during winter needle sampling campaigns (December until March). Sample preparation procedure typically includes separation of needle age classes, drying, milling and chemical analyses for macronutrients and further drying of a subsample at 105°C to constant weight for the determination of dry weight. The participating ICP Forests countries harvested and carried out these preprocessing steps and collected the associated metadata. Hg measurements of samples from ICP Forests Level II plots were performed at the University of Basel. Additional foliar Hg concentration data of 1440 samples from the Austrian Bio-Indicator Grid organized by the Austrian Federal Research Center for Forests (German acronym BFW) (Austrian Bio-Indicator Grid) were included in the analysis. The combined dataset consists of 3,569 foliage samples encompassing 23 species of coniferous and deciduous trees (Table S1). The most frequent (number of samples > 100) species within the dataset are Norway spruce (*Picea abies*; n = 2073), Scots pine (*Pinus sylvestris*; n = 413), European beech (*Fagus sylvatica*; n = 372), silver fir (*Abies alba*; n = 162), sessile oak (*Quercus petraea*; n = 133), Austrian pine (*Pinus nigra*; n = 125) and common oak (*Quercus robur*; n = 101). We pooled individual tree species into groups of tree species genera (e.g. beech, oak, pine, spruce), see Table S1. Coniferous samples consist of needles of different age classes: most of the needle samples (n = 1958) flushed in the sampling season (current season; y_0), 600 samples are one-year old (y_1), 121 samples are two-year old (y_2), 125 are three-year old (y_3), 22 samples are four-year old (y_4), 60 samples are five-year old (y_5) and 3 samples are six-year old (y_6) needles. All data analysis of this study concerning tree species, foliage structure, nutrient contents and meteorological and site-specific parameters (Sect. 3.1 – 3.6) is based on Hg values of current-season (y_0) foliage. Foliage samples originate from 995 European sites: 232 sites are ICP Forests Level II forest monitoring plots, 737 locations are

sampling sites of the Austrian Bio-Indicator grid and the remaining sites (26) are not classified within the ICP Forests program. See Figure 1 for a geographic overview of foliage sampling sites from the sampling year 2017.
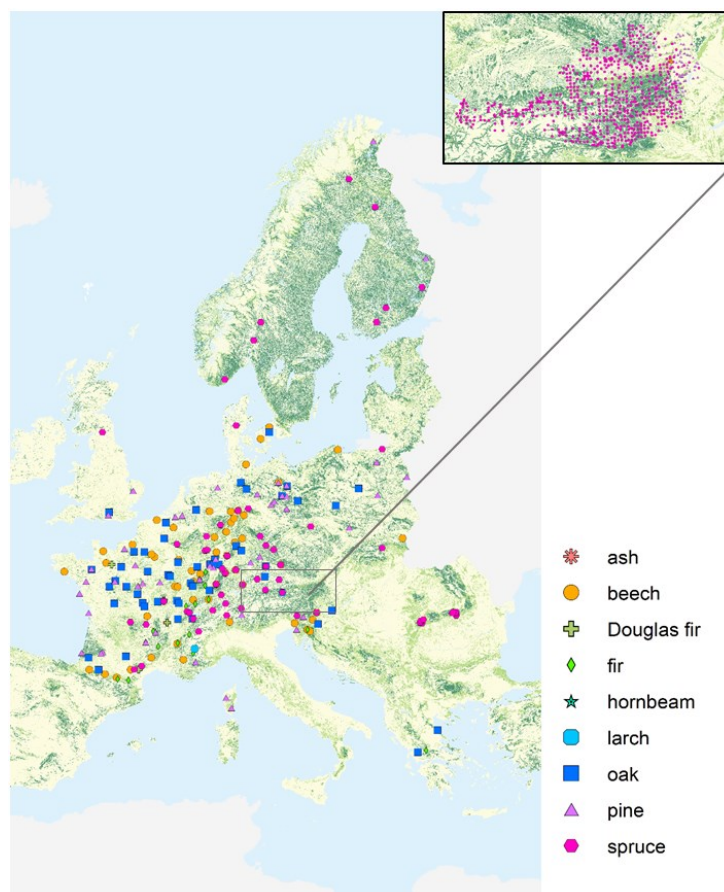
135

Figure 1. Overview of forest plots, at which Hg foliage samples were harvested from different tree species groups during the sampling year 2017. At around 12% of plots in 2017, foliage from more than one tree species group was sampled. Geographic distribution of sampling sites in 2015 is similar, except there were no samples from the ICP Forests partners Brandenburg (Germany), Baden-Württemberg (Germany) and Poland and there were samples from five additional plots in North Rhine-Westphalia (Germany), see Fig. S1.
140   The enlarged map view at the top right depicts sampling locations of the Bio-Indicator Grid in Austria in 2015 and 2017. Use of base map authorized under European Commission reuse policy (EU, 2011).

We assembled the foliar Hg concentration dataset including the following metadata: sampling date, needle age class, leaf mass per area (LMA; 19% of samples), drying temperature, leaf nitrogen (N) and organic carbon (C_{org}) concentration. Foliage
145   concentrations of N and C_{org} were measured in laboratories in respective ICP Forests countries following strict QA procedures. The tolerable quality limit for N concentration measurements is ± 15% (for N concentration > 5 mg g^{-1}) of the mean inter-laboratory N concentration in foliar reference material distributed for ICP Forests laboratory comparison tests (Rautio et al., 2016).

The measurements and observation from ICP Forests Level II forest plots additionally included the beginning of the growing season for the sampling years 2015 and 2017 (where available) (Vilhar et al., 2013), main tree species on the plot, mean age of trees on the plot (estimated during system installment), basal area and trees per hectare on the plot (Dobbertin and Neumann, 2016), soil texture of the upper soil layer (mineral soil between 0 – 5 cm or 0 – 10 cm from the survey years 2003 - 2019) (Fleck et al., 2016; Cools and De Vos, 2020) as well as altitude and geographic coordinates. At the tree level, meta data consist of tree species, tree number and diameter at breast height (Dobbertin and Neumann, 2016). Meteorological in-situ measurements of hourly temperature and relative humidity (Raspe et al., 2013) were available for 82 forest Level II plots for both 2015 and 2017.

Furthermore, we amended the dataset with satellite-based values of transpiration from the Global Land Evaporation Amsterdam Model (GLEAM) (Miralles et al., 2011; Martens et al., 2017), of hourly soil water (layer 1, 0 – 7 cm) and surface air temperature (2 m height) from ERA5-Land (Muñoz Sabater, 2019) for the respective regions of every forest plot. GLEAM (v. 3.3a) data were available at daily resolution and on a 0.25° latitude-longitude regular grid. ERA5-Land values were available at hourly resolution and on a 0.1° latitude-longitude regular grid. For each forest plot, we calculated average daily GLEAM (v.3.3a) transpiration within the life period of foliage samples, from the beginning of the growing season to harvest. Similarly, from ERA5-Land values, we calculated the average 2 m air temperature within respective sample life periods. We detected outliers of time-normalized foliar Hg concentrations (see Sec. 2.3) within each tree species and needle age class by applying the modified Z score method according to Iglewicz and Hoaglin (1993) using an absolute threshold value of 3.5, above which a modified Z score value was considered an outlier. As a result, 3.2% of values within the dataset were removed as outliers.

2.2 Correction of foliar Hg concentrations for drying temperature

Drying and grinding of foliage samples were carried out by ICP Forests laboratories and BFW. All foliar concentration values (Hg, N and C_{org}) within the dataset are normalized to dry weight for a sample drying temperature of 105 °C in order to make values internally consistent. The actual drying temperature differed between foliage samples (40 °C – 80 °C). In order to adjust for actual drying temperature, the laboratories determined the drying factor to correct for water content of each sample by drying an aliquot of foliage sample at actual drying temperature and subsequently at 105 °C. The drying factor was available for 62% of samples within the dataset. For the rest of the samples an average drying factors per tree species and needle age class was applied for drying temperature correction. Smallest average drying factor was 1.03 ± 0.003 (mean ± sd) for one-year old (y_1) *Pinus pinaster* needles and biggest average drying factor was 1.07 ± 0.02 (mean ± sd) for *Quercus robur* leaves. Previous studies did not detect Hg losses with drying temperature in foliage (Wohlgemuth et al., 2020; Pleijel et al., 2021), wood (Yang et al., 2017) or moss (Lodenius et al., 2003).

2.3 Foliage Hg analysis

180   Total Hg concentrations in foliage samples from ICP Forests Level II plots were measured at the University of Basel using a direct mercury analyzer (Milestone DMA-80, Heerbrugg, Switzerland). Standard operation procedure involved measuring a pre-sequence of four blanks (three empty sample holders and wheat flour) and three liquid primary reference standards (50 mg of 100 ng g^{-1} NIST-3133 in 1% BrCl). If the three liquid primary reference standards were within 90% - 110% of expected value, we corrected all measurement results of the respective sequence accordingly. Otherwise, we discarded the sequence and

185   re-calibrated the instrument. Standard reference materials (SRM) (NIST-1515 apple leaves and spruce needle sample B from the 19th ICP Forests needle/leaf interlaboratory comparison test) were measured in each sequence (4 SRM in a sequence of 40 samples) and the sequence was discarded, if the measured SRM value was outside the certified uncertainty range (NIST-1515) or outside ± 10% of the expected concentration (ICP Forests spruce B). Absolute Hg content in wheat blanks within the sequence had to be < 0.3 ng. We successfully participated in the 21st (2018/2019), 22nd (2019/2020) and 23rd (2020/2021) ICP

190   Forests needle/leaf interlaboratory comparison (ILC) test. Total Hg concentrations in foliage samples from the Austrian Bio-Indicator Grid were measured using a Hg analyzer (Altec-AMA 254 HCS, Prague, Czech Republic). Standard operation procedure at BFW involved a pre-sequence of five blanks (empty nickel boats) and measurements of three samples of reference material (BCR-62 olive leaves or spruce needle samples from the 17th or 19th ICP Forests needle/leaf ILC test) after every 40th sample within a sequence. If the measurement results of the three reference samples were outside of 93% - 107% of expected

195   value, a drift correction was performed. Final foliage Hg concentrations within the Bio-Indicator Grid represent average values of at least two replicates.

2.4 Determination of the beginning of the growing season for calculating daily foliage Hg uptake rates

Mercury concentrations in leaves and needles have been demonstrated to increase linearly over the course of the growing season (Rea et al., 2002; Laacouri et al., 2013; Blackwell et al., 2014; Wohlgemuth et al., 2020). In this study, foliage samples

200   within the data set were harvested at various points in time, making a direct comparison of measured Hg concentrations unfeasible. We therefore calculated foliar Hg uptake rates (in ng Hg g$^{-1}_{d.w.}$ d^{-1}) of current-season samples by normalizing foliar Hg concentrations to their respective life period in days from the beginning of the growing season (emergence of new foliage) to date of harvest. These resulting foliar Hg uptake rates are net Hg accumulation rates per gram dry weight on a leaf basis and should not be confused with foliar Hg fluxes on a whole-tree basis. Please also note, that daily foliar Hg uptake rates in this

205   study represent average values over the growing season. The actual daily foliar Hg uptake on a given day might differ from the average value depending on the time period within the growing season (e.g. early season vs. peak season) (Laacouri et al., 2013). Needles of age 1 year or older were excluded from calculating daily foliage Hg uptake fluxes, since Hg uptake might slow down in physiologically less active older needles (Wohlgemuth et al., 2020) and it is unclear, to which extend Hg uptake occurs in older needles in winter and in early spring before the emergence of new foliage. While dates of harvest were available

210   for all samples, we determined the start of the growing season of current-season foliage by combining available data sources

with start-of-season modelling. These data sources comprise in-situ phenological observations, which were available for 15% of samples, and observations of the emergence of current-season needles of coniferous tree species from the Pan European Phenological database PEP725 (Templ et al., 2018). We assigned observations from PEP725 to the corresponding closest forest plot of the respective sampling year (2015 or 2017) by using the nearest neighbor function *matchpt* from the Biobase package in R (Huber et al., 2015), such that differences between PEP725 observation and forest plots did not exceed 3° in latitude, 30 m in altitude and closely matched longitude as possible. For details on the matching procedure and results see supplementary information, Sect. S3.1. To model the beginning of the growing season for deciduous trees, we utilized the leaf area index (LAI) product by Copernicus Global Land Service based on PROBA-V satellite imagery at a resolution of 300 m and 10 days (Dierckx et al., 2014; Fuster et al., 2020) following a recommendation by Bórnez et al., 2020. For information on the model and quality assurance, refer to supplementary information, Sect. S3.2.

2.5 Evaluation of data on water vapor pressure deficit (VPD)

At 82 ICP Forests Level II plots (in total from both years 2015 and 2017), in-situ meteorological data at an hourly resolution were recorded in 2015 and 2017, for which we calculated hourly water vapor pressure deficit (VPD) values at daytime (06:00 – 18:00 LT). The VPD represents the difference between the water vapor pressure at saturation and the actual water vapor pressure. We calculated saturated water vapor pressure from average hourly air temperature using the August-Roche-Magnus formula (Yuan et al., 2019) and actual water vapor pressure as the saturation water vapor pressure multiplied by the average hourly relative humidity. These VPD values were calculated exclusively for daytime hours (06:00-18:00 LT), because both $Hg(0)$ and photosynthetic CO_2 uptake by trees are at maximum during the day (Obrist et al., 2021). From these daytime hourly VPD values at each forest plot, we calculated the proportion of hours within the daytime life period of the samples (from the beginning of the growing season to sampling day), during which VPD exceeded the four threshold values of 1.2 kPa, 1.6 kPa, 2 kPa and 3 kPa, respectively. We chose these four VPD thresholds as test values because they were reported in literature to incrementally induce leaf stomatal closure of temperate forest trees, ranging from initial stomatal closure (around 0.8 kPa – 1 kPa (Körner, 2013)) to maximum stomatal closure (at around 3 kPa – 3.2 kPa (CLRTAP, 2017)). We calculated the average proportion of daily daytime exceedance hours of VPD > respective threshold value by normalizing total number of respective daytime VPD exceedance hours with total number of daytime hours during the corresponding sample life period.

2.6 Evaluation of ERA5-Land volumetric soil water contents

We calculated the time proportion within sample life periods, during which the volumetric soil water content in the region of the respective forest plots fell below a soil texture dependent threshold value (PAW_{crit}) where plants are expected to close their stomata due to limited water availability. To this, we used the satellite-derived ERA5-Land data of hourly soil water in soil layer 1 (vertical resolution: 0 – 7 cm, horizontal resolution: 0.1° x 0.1°) (Muñoz Sabater, 2019) and data on soil texture of the

respective forest plots, where available (Fleck et al., 2016). Field data from literature suggest, that plant stomata start to close, once the plant available water (PAW) in the soil falls below a critical value (PAW_{crit}) (Domec et al., 2009; Grünhage et al., 2011, 2012). The soil PAW represents the difference between soil water at field capacity (SW_{FC}) and soil water at the permanent wilting point (SW_{PWP}). We calculated $PAW_{crit} = 0.5 \times PAW + SW_{PWP}$ following a recommendation by Büker et al. (2012 and used PAW_{crit} as the threshold value to calculate the proportion of hours within the respective sample life periods, during which soil water $< PAW_{crit}$. See Figure S11 for an exemplary time series of ERA5 soil water in the region of a forest plot in France in 2015. Soil texture specific values for SW_{FC} and SW_{PWP} (Table S4) were obtained from Saxton and Rawls (2006).

3 Results and Discussion

3.1 Variation of foliar Hg concentrations with foliar life period

Average foliar Hg concentrations (mean ± sd) differed between tree species groups (see Table S1 for definition of tree species groups). Ash leaves exhibited highest Hg concentrations (32.2 ± 5.7 ng Hg $g^{-1}_{d.w.}$; n = 10), followed by beech leaves (25.5 ± 9.6 ng Hg $g^{-1}_{d.w.}$; n = 372), current-season Douglas fir needles (22.9 ± 6.7 ng Hg $g^{-1}_{d.w.}$; n = 27), hornbeam leaves (32.2 ± 5.7 ng Hg $g^{-1}_{d.w.}$; n = 10), oak leaves (20.8 ± 9.1 ng Hg $g^{-1}_{d.w.}$; n = 287), larch needles (13.4 ± 3.4 ng Hg $g^{-1}_{d.w.}$; n = 3), current-season spruce needles (11.8 ± 3.4 ng Hg $g^{-1}_{d.w.}$; n = 1509), current-season fir needles (11.4 ± 2.8 ng Hg $g^{-1}_{d.w.}$; n = 66) and current-season pine needles (11.0 ± 5.1 ng Hg $g^{-1}_{d.w.}$; n = 344). For all tree species sampled at more than 20 forest plots, we found significant ($p < 0.05$) positive trends of foliar Hg concentrations with respective sampling date within the growing season (see Figure 2 for beech and oak and Fig. S4 for pine and spruce).
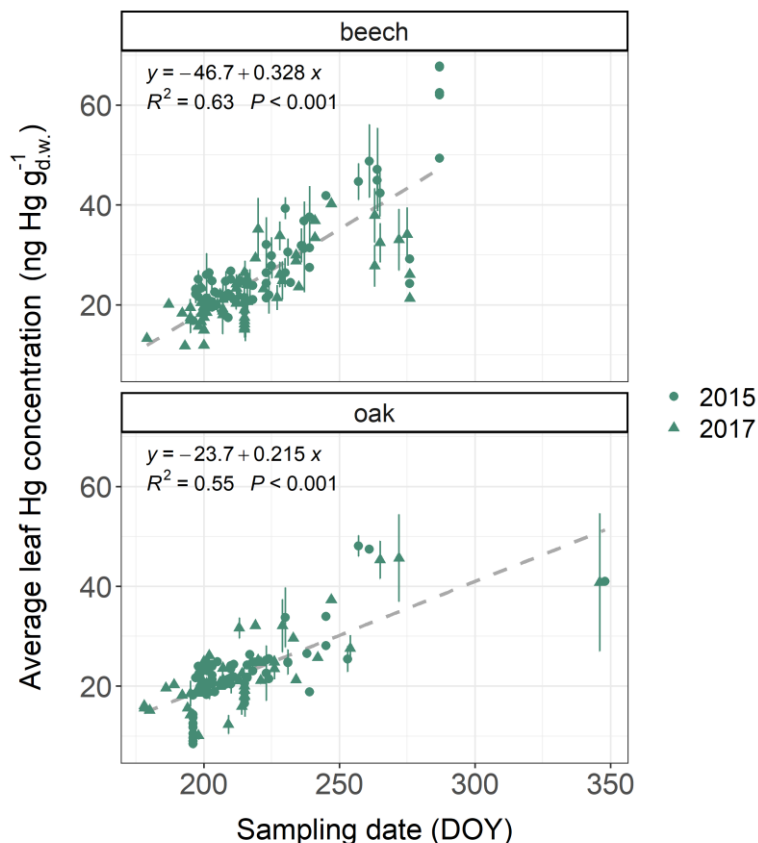
Figure 2. Average leaf Hg concentrations (ng Hg g^{-1}$_{d.w.}$) in beech and oak samples at multiple ICP Forests plots versus sampling dates (day of year; DOY) of respective samples. Sampling took place both in 2015 and 2017. Two plots of holm oak (*Quercus ilex*) are located in Greece and were sampled in December 2015 (DOY = 348) and December 2017 (DOY = 346). Error bars denote ± one standard deviation between multiple samples at each forest plot.

Increasing foliar Hg concentrations with progressing sampling date are in line with previous observations demonstrating that at individual sites Hg concentrations increased linearly over the growing season (Rea et al., 2002; Laacouri et al., 2013; Wohlgemuth et al., 2020; Pleijel et al., 2021). To make Hg levels in foliage sampled at different times comparable, we calculated daily foliar Hg uptake rates by normalizing foliar Hg concentrations with the life period of samples. These daily foliar Hg uptake rates represent average values over the life period. The average life period (mean ± sd) of samples was 104 d ± 30 d for beech, 104 d ± 24 d for oak, 159 d ± 12 d for pine and 148 d ± 14 d for spruce. At five percent of spruce plots sampling took place in winter (December until March). Spruce and pine trees have been found to reduce their physiological activity (transpiration, net photosynthesis) at low soil temperatures (< 8 – 10 °C), potentially impacting stomatal Hg(0) uptake in winter (Schwarz et al., 1997; Mellander et al., 2004). The average daily Hg uptake rates of current-season spruce needles sampled during peak season (0.084 ng Hg g^{-1}$_{d.w.}$ day^{-1}) and sampled during winter (0.067 ng Hg g^{-1}$_{d.w.}$ day^{-1}) were significantly different (Welch two sample t-test; p = 0.015 at 95% confidence level). If spruce trees continue to accumulate Hg throughout

the winter, Hg needle concentrations should be higher in winter samples than in samples harvested earlier during the growing season and Hg uptake rates per day should be comparable between winter and growing season samples. Thus, the difference of average daily Hg uptake between winter and growing season spruce needle samples indicates a decrease of Hg accumulation in spruce needles during winter. However, the potential of needle Hg uptake in winter needles requires further investigation, e.g. by performing a full winter sampling at multiple forest plots. For this study, we shortened the calculated life period of spruce needles from winter sampling plots to 15th November (Rötzer and Chmielewski, 2001) to improve comparability of spruce needle Hg uptake rates within the dataset.

3.2 Variation of foliar Hg uptake rates with tree species groups

Median daily foliar Hg uptake rates (Fig. 3) in decreasing order are: ash (0.26 ng Hg $g^{-1}_{d.w.}$ d^{-1}), beech (0.25 ng Hg $g^{-1}_{d.w.}$ d^{-1}), oak (0.22 ng Hg $g^{-1}_{d.w.}$ d^{-1}), hornbeam (0.20 ng Hg $g^{-1}_{d.w.}$ d^{-1}), larch (0.14 ng Hg $g^{-1}_{d.w.}$ d^{-1}), current-season Douglas fir needles (0.13 ng Hg $g^{-1}_{d.w.}$ d^{-1}), current-season spruce needles (0.07 ng Hg $g^{-1}_{d.w.}$ d^{-1}), current-season fir needles (0.07 ng Hg $g^{-1}_{d.w.}$ d^{-1}) and current-season pine needles (0.05 ng Hg $g^{-1}_{d.w.}$ d^{-1}). The range of daily foliar Hg uptake of beech (0.12 – 0.42 ng Hg $g^{-1}_{d.w.}$ d^{-1}) is in agreement with the daily foliar Hg uptake rate of 0.35 ± 0.03 ng Hg g^{-1} d^{-1}, that Bushey et al. (2008) had determined in beech leaves growing in New York State in 2005. There are distinct differences in median daily Hg uptake rates between current-season foliage of tree species groups (Fig. 3). The median daily foliar Hg uptake rate of deciduous leaf samples is 0.23 ng Hg $g^{-1}_{d.w.}$ d^{-1}, a factor of 3.2 larger than the median daily foliar Hg uptake rate of current-season conifer needle values (0.07 ng Hg $g^{-1}_{d.w.}$ d^{-1}). The difference between deciduous and coniferous leaves in the European dataset is smaller than a previous observation from a mixed forest site in Switzerland in 2018, where Hg uptake rates of coniferous species were reported to be 5 times lower than those of deciduous trees (Wohlgemuth et al., 2020). Similarly, Navrátil et al. (2016) reported higher foliar Hg concentrations in beech leaves (36.3 ng Hg g^{-1}) than in current-season spruce needles (14.1 ng Hg g^{-1}) of two adjacent forest plots sampled during peak season (August). Higher Hg concentrations in deciduous leaves (median: 28 ng Hg g^{-1} from 341 remote sites) than in composite multi-age coniferous needles (median: 15 ng Hg g^{-1} from 535 remote sites) were also reported in a global literature compilation (Zhou et al., 2021). Differences in daily foliar Hg uptake between tree species within one genus (e.g. *Quercus petraea* and *Quercus robur*) were negligible (see Fig. S5). We were not able to normalize daily foliar Hg uptake rates with atmospheric Hg(0) concentrations at each respective sampling site and sample life period, as air Hg(0) measurements were unavailable for our sampling sites. The relative standard deviation of average air Hg(0) concentrations at 6 European measurement sites within the EMEP network (Tørseth et al., 2012; EMEP, 2021) between May and Sept. 2015 and 2017 (see Table S2 for details) was 0.06, which is lower than the relative standard deviation of the average daily Hg uptake rates between tree species and forest plots of 0.64 (Figure 3). We therefore argue, that the pronounced differences in median daily foliar Hg uptake rates between tree species cannot exclusively be explained by differences in atmospheric Hg(0) concentrations, but rather suggest a tree physiological cause. However, foliar Hg uptake rates should be normalized to ambient atmospheric Hg(0) concentrations, in particular when comparing foliar Hg observation between the northern and southern Hemisphere or over multi-decadal timescales.
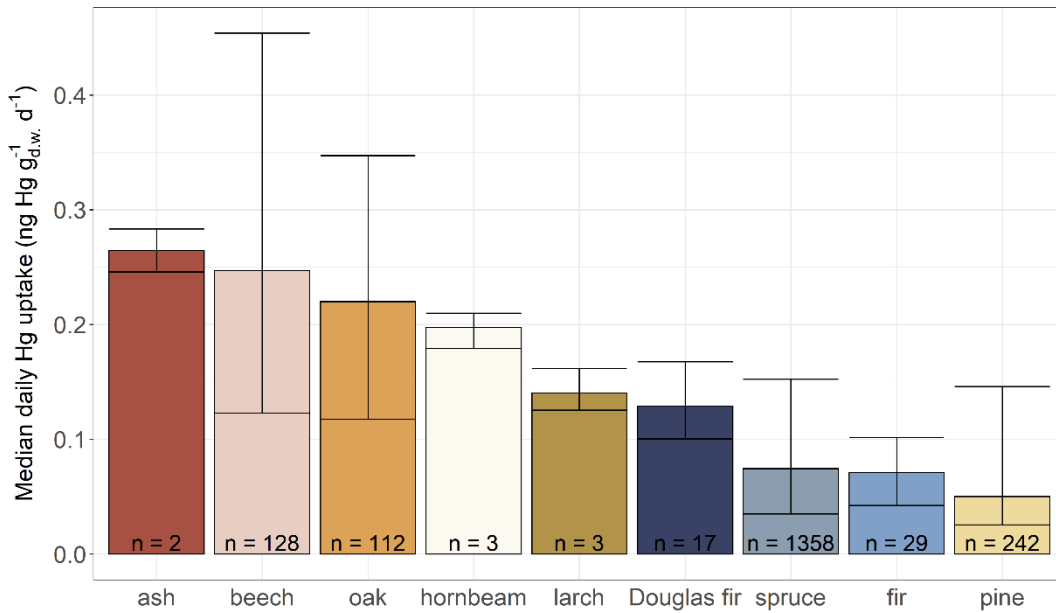
310 **Figure 3.** Median daily foliar Hg uptake (ng Hg g^{-1}$_{d.w.}$ day^{-1}) between different tree species groups (see Table S1 for definition of tree species groups) arranged from highest to lowest value. Error bars give the value range within each tree species group and n indicates the number of sites at which the respective tree species were sampled in both the years 2015 and 2017. Foliar samples of evergreen coniferous tree species (Douglas fir, spruce, fir and pine) consist of needles of the current season.

3.3 Foliar Hg uptake and sample-specific N concentration

315 Foliar N concentration serves as a surrogate for the maximum photosynthetic capacity of foliage (Reich et al., 1998) as the bulk amount of foliar N is contained in the photosynthetic systems like chlorophylls, thylokoid proteins and rubisco (Evans, 1989; Körner, 2013; Loomis, 1997). Furthermore, foliar N represents an indirect proxy for foliar maximum stomatal diffusive conductance for water vapor, independent of tree species (Körner et al., 1979; Bolton and Brown, 1980; Schulze et al., 1994; Reich et al., 1999; Meziane and Shipley, 2001; Körner, 2013, 2018). Note, that for this analysis we solely compared N and Hg

320 concentrations for foliage samples harvested within a period of the growing season, during which leaf N concentrations are relatively stable (July – August for broadleaves (Wilson et al., 2000; Mediavilla and Escudero, 2003) and Sept – March for conifer needles (Adams et al., 1987; Hatcher, 1990)). To assess the possibility of physiological factors controlling the large variation of foliar Hg(0) uptake between different tree species groups (Fig. 3), we compared average daily foliar Hg uptake rates per tree species group with respective average foliar N concentrations. We found a positive linear correlation between

325 foliar N concentration and Hg uptake rates as tree species groups with high average foliar N exhibited higher daily foliar Hg uptake rates (Table 1). This observation supports the notion, that the physiological activity of trees controls foliar Hg(0) uptake, thereby explaining the large variation among tree species groups (Wohlgemuth et al., 2020). We compared foliar Hg uptake rates and leaf N concentrations with values of median stomatal conductance for beech, oak, pine and spruce included in a global leaf-level gas exchange database compiled by Lin et al. (2015) (see description of database calculation in Sect. S7).

330   Albeit stomatal conductance measurements for tree species of interest within the database (Lin et al., 2015) originated from one or only few sites (n = 1 – 5; Table 1), beech and oak exhibited higher median stomatal conductance values than spruce and pine, corresponding with higher daily Hg uptake rates and foliar N concentrations in beech and oak compared to spruce and pine. Thus, we observed a strong control of plant functional traits on foliar Hg(0) uptake with tree species of high photosynthetic activity (high N concentration) and stomatal conductance exhibiting the highest foliar Hg(0) uptake rates.

335

Table 1: Mean ± standard deviation of daily Hg uptake and foliar N concentration per tree species group from a subset of foliage samples harvested during July – Aug (broadleaf samples) or Sept – March (coniferous needle samples). Values are ordered from highest to lowest mean daily Hg uptake. All values from evergreen tree species groups (Douglas fir, fir, pine, spruce) were evaluated in current-season needles. Median stomatal conductance values (min – max) were calculated from a global database of leaf-level gas exchange parameters compiled
340   by Lin et al. (2015).

Tree species group	daily Hg uptake ($ng\ Hg\ g^{-1}_{d.w.}\ d^{-1}$)			foliar N conc. ($mg\ N\ g^{-1}_{d.w.}$)			n samples	median stomatal conductance ($mol\ m^{-2}\ s^{-1}$) (Lin et al., 2015)	n sites (Lin et al., 2015)
beech	0.25	±	0.05	23.1	±	2.9	312	0.10 (0.03 – 0.31)	2
oak	0.20	±	0.05	25.1	±	2.8	252	0.15 (0.01 – 0.35)	1
hornbeam	0.19	±	0.03	19.4	±	2.1	10		
Douglas fir	0.13	±	0.02	17.0	±	3.5	26		
spruce	0.08	±	0.02	12.9	±	1.7	1509	0.05 (0.01 – 0.16)	1
fir	0.07	±	0.02	13.0	±	1.7	66		
pine	0.06	±	0.02	14.4	±	3.0	355	0.06 (0.00 – 0.33)	5

    Within tree species groups, linear regression coefficients of daily Hg uptake and foliar N concentration were significant ($p <$ 0.001) for beech (R^2 = 0.15; n = 312) and fir (R^2 = 0.27; n = 66). Corresponding statistical significance for hornbeam, oak,
345   pine and spruce could not be evaluated, since the respective data used for the linear regression was heteroscedastic. Blackwell and Driscoll (2015) found a significant relationship between foliar Hg concentration and foliar N% for yellow birch, sugar maple and American beech, but not for pine (red pine and white pine), red spruce or balsam fir. We examined whether unaccounted site-specific differences (e.g. soil N concentration) between forest plotscould have caused the variability (low R^2) of daily Hg uptake versus foliar N concentration within tree species by individually analyzing foliar Hg concentration versus
350   foliar N concentration at two oak and one beech forest plot, from which 20 or more foliage samples were available. Linear regression coefficients of foliar Hg concentrations versus foliar N concentrations were significant ($p <$ 0.001) at two (oak and beech) of the three plots but not at the third plot ($p =$ 0.1, oak) (see Fig. S7). This finding suggests that foliar N concentrations

represents an indicator of foliar Hg concentrations at individual forest sites, as it does for foliar Hg uptake of different tree species (Table 1). However, given the heterogeneity of nutrient availability between sites (Vesterdal et al., 2008) and the complexity of internal foliar allocation of N to different parts of the photosynthetic apparatus (Hikosaka, 2004), a generally valid correlation of foliar Hg uptake versus foliar N may not exist.

3.4 Foliar Hg uptake and Leaf Mass per Area

Within the whole dataset, leaf mass per area (LMA; $g_{d.w.}$ m^{-2}_{leaf}) data were available in a subset of 349 foliage samples from 48 sites (from both 2015 and 2017). LMA is an important parameter in plant ecophysiology, because carbon gains of plants via photosynthetic activity and gas diffusion is optimized per unit of leaf area, as plants adapt their LMA, i.e. their foliage thickness and/or tissue density, to the availability of sunlight during growth (Ellsworth and Reich, 1993; Niinemets and Tenhunen, 1997; Rosati et al., 1999). This LMA adaptation of foliage to sunlight had been suggested to be more effective for optimizing photosynthetic capacity than within-leaf N partitioning of photosynthesizing biomass (Evans and Poorter, 2001). Therefore, we analyzed the connection of foliar Hg uptake to LMA across tree species. Figure 4 shows average LMA values (mean ± sd) of the subset of samples where LMA was reported, resolved by tree species, along with respective average daily Hg uptake rates and associated foliar N concentrations (all values displayed in Fig. 4 are listed in Table S3; see Fig. S8 for density plots of datasets from Table 2 and Fig. 4).
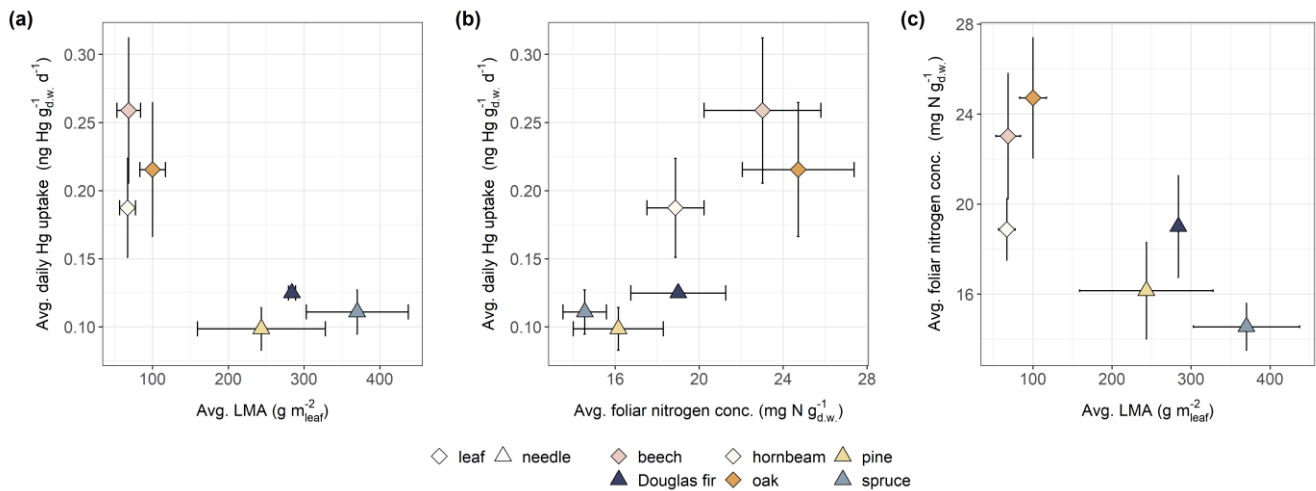
Figure 4. a) Average daily Hg uptake rates (ng Hg $g^{-1}_{d.w.}$ d^{-1}), b) average foliar nitrogen concentrations (mg N $g^{-1}_{d.w.}$) and c) average LMA ($g_{d.w.}$ m^{-2}_{leaf}) determined in 349 foliage samples and resolved by tree species group and foliage type (leaf/needle). Error bars denote ± one standard deviation. Number of samples (n) differs between tree species: beech (n = 164), Douglas fir (n = 2), hornbeam (n = 9), oak (n = 106), pine (n = 35) and spruce (n = 33).

Current-season needle samples of coniferous tree species groups (Douglas fir, pine, spruce) exhibited higher median LMA values (308 $g_{d.w.}$ m^{-2}_{leaf}), lower median daily Hg uptake rates (0.10 ng Hg $g^{-1}_{d.w.}$ d^{-1}) and lower median foliar N concentrations (15.4 mg N $g^{-1}_{d.w.}$) compared to leaf samples of deciduous tree species groups (beech, oak, hornbeam) (Fig. 4). Wright et al.

(2004) illustrated, that different evolutionary survival strategies of plant species are positioned along a single axis of foliage characteristics ranging from plant species with high photosynthetic capacity and respiration, high foliar N concentration, low LMA and short leaf life spans to plant species with the respective opposite attributes. Comparison of average daily foliar Hg uptake, LMA and foliar N concentrations (Fig. 4) across tree species in this study suggest, that foliar Hg(0) uptake aligns along this plant species economics spectrum, with deciduous leaves with high leaf N concentrations and thus high physiological capacity (photosynthesis, respiration) taking up more Hg(0) per gram dry weight over the same time span than coniferous needles with low leaf N concentrations and physiological capacity.

3.5 Foliar Hg uptake and water vapor pressure deficit (VPD)

Trees regulate their transpiration rates in response to temporary changes of water vapor pressure deficit (VPD) by controlling leaf stomatal aperture (Franks and Farquhar, 1999; McAdam and Brodribb, 2015; Grossiord et al., 2020). When a critical VPD threshold is exceeded, trees close their stomata to resist cavitation and excessive water loss in conditions of high atmospheric evaporative forcing (i.e. high VPD) (Körner, 2013; Grossiord et al., 2020). This decrease in leaf stomatal conductivity in response to high VPD suppresses stomatal uptake fluxes of gaseous pollutants like ozone (Emberson et al., 2000; Körner, 2013). We investigated, whether VPD impacts foliar uptake of gaseous Hg(0) by relating species-specific average daily foliar Hg uptake rates to the proportion of daytime (06:00 – 18:00 LT) hours of an average day within the respective sample life periods, during which hourly daytime VPD exceeded the threshold values of 1.2 kPa, 1.6 kPa, 2 kPa and 3 kPa, respectively at all forest plots with hourly meteorological data (n = 82 including both sampling years).
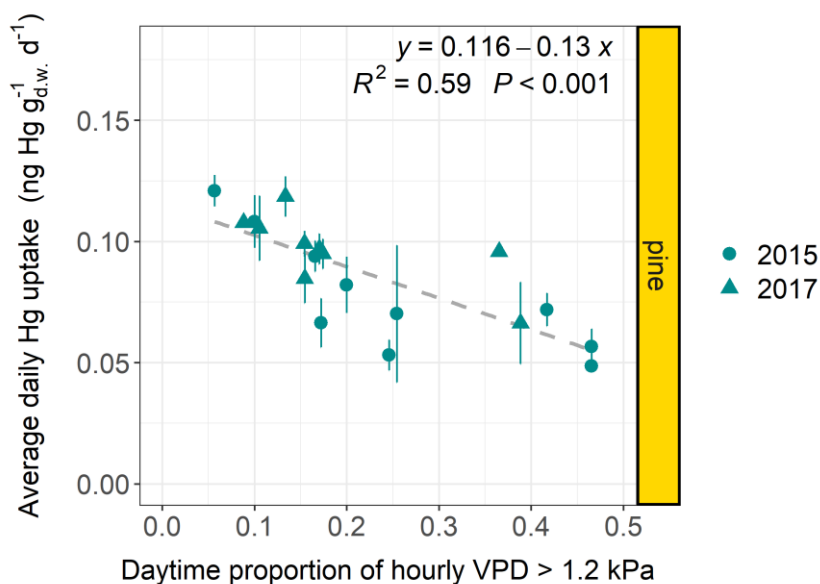
Figure 5. Average daily Hg uptake rates (ng Hg $g^{-1}_{d.w.}$ d^{-1}) of current-season pine needles from multiple forest plots (n plots = 19) versus the proportion of daytime hours (06:00 – 18:00 LT) within an average day of the respective sample life periods, during which the hourly daytime water vapor pressure deficit (VPD) exceeded a threshold value of 1.2 kPa. Data points originate from both sampling years 2015 and 2017. All forest plots are located in Central Europe (latitude 46° - 54°), for which ambient air Hg(0) concentrations are relatively constant (see

Table S2 and Fig. S6). Error bars denote ± one standard deviation of daily needle Hg uptake rates between multiple samples at each forest plot.

400   The linear regression coefficients of average daily Hg uptake versus daily proportion of daytime hours, during which VPD exceeded a threshold value (1.2 kPa, 1.6 kPa, 2 kPa or 3 kPa) were significant ($p < 0.01$) for pine at all VPD threshold values (Fig. 5, Fig. S9), for spruce at a VPD threshold value of 3 kPa ($R^2 = 0.44$; $p = 0.01$; $n = 14$) (Fig. S9) and not significant for beech and oak at any VPD threshold value (Fig. S10). Linear regression coefficients were negative for all species and VPD threshold values, i.e. by tendency, average daily foliar Hg uptake rates decreased with average proportion of daytime hours,

405   during which VPD > respective threshold value (1.2 kPa, 1.6 kPa, 2 kPa or 3 kPa). We excluded Douglas fir, fir, hornbeam and larch from the regression analysis due to a low number of forest plots ($n = 1 – 5$). Average daily needle Hg uptake rates of spruce needles were clustered between two groups of forest plots with high and low daytime proportions of VPD > threshold (Fig. S9) relative to each other. T-test revealed a significant ($p = 0.008$) difference in average daily spruce needle Hg uptake rates between the two clusters for a VPD threshold value of 3 kPa and non-significant ($p > 0.05$) differences for all other VPD

410   threshold values. The timing and degree of stomatal closure during dry conditions is tree species-specific (Zweifel et al., 2009; Tsuji et al., 2020). Tree species like pine and spruce are isohydric, i.e. they tend to respond to drought stress under high evaporative demand by closing their stomata earlier than anisohydric species like beech and oak (Martínez-Ferri et al., 2000; Zweifel et al., 2007; Carnicer et al., 2013; Coll et al., 2013; Cárcer et al., 2018). Among isohydric species, pine has been discovered to reduce tree conductance and stomatal aperture during the onset of dry conditions earlier and at a greater rate than

415   spruce (Lagergren and Lindroth, 2002; Zweifel et al., 2009). Spruce has been observed to keep stomata almost completely closed under drought stress, i.e. high VPD and/or soil water deficit (Zweifel et al., 2009). We hypothesize, that the significantly decreasing average foliar stomatal Hg uptake rates with daytime proportion of VPD > 1.2 kPa for pine (Fig. 5) and of VPD > 3 kPa for spruce (Fig. S9) possibly reflect the early physiological response of pine, and the high degree of stomatal closure under drought stress of spruce. Oak exhibits later stomatal closure at the onset of dry conditions and higher stomatal aperture

420   under drought stress than e.g. pine (Zweifel et al., 2007, 2009), which may be the reason why there was by tendency a negative, but not significant correlation coefficient of average foliar Hg uptake with daytime proportion of VPD > any threshold value for oak (Fig. S10).

3.6 Foliar Hg uptake and soil water content

    Linear regression coefficients of average daily foliar Hg uptake rates at each forest plot versus proportion of hours within

425   sample life periods, during which ERA5-Land soil water fell below a soil texture specific threshold value (PAW_{crit}) (see Sect. 2.6), were negative for all tree species groups and significant for beech ($p = 0.036$) and pine ($p = 0.031$) (Fig. 6). The linear regression coefficient was not significant for oak ($p = 0.169$) and not available for spruce due to a low number of data points.
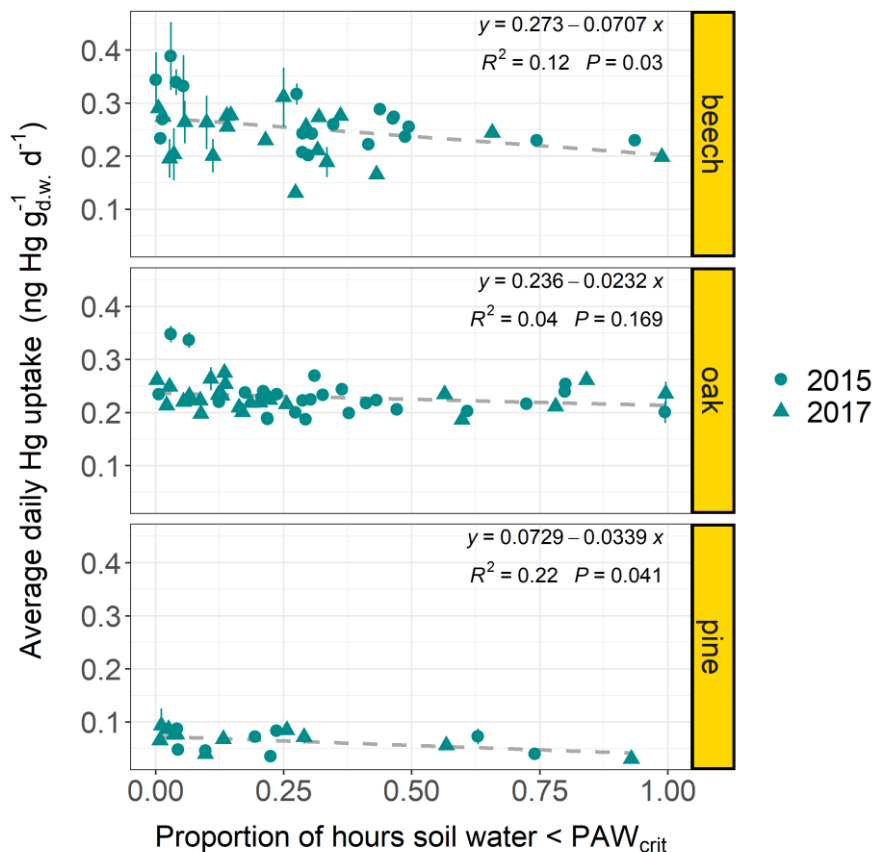
Figure 6. Average daily Hg uptake rates (ng Hg $g^{-1}_{d.w.}$ d^{-1}) of beech, oak and current-season pine foliage from multiple forest plots (beech plots n = 38; oak plots n = 45; pine plots n = 19; latitude: 41° - 55°) versus the proportion of hours within the respective sample life periods, during which the geographically associated hourly soil water from the ERA5-Land dataset (Muñoz Sabater, 2019) fell below a soil texture specific threshold value PAW_{crit} (see Sect. 2.6). Data points originate from both sampling years 2015 and 2017. Error bars denote ± one standard deviation of daily needle Hg uptake rates between multiple samples at each forest plot.

Linear regression results (Fig. 6) indicate, that foliar Hg uptake rates decrease at forest plots, where plant available water in the upper soil layer (0 – 7 cm) falls below specific thresholds (PAW_{crit}) for a relatively long time period over the growing season. Studies on the atmosphere-plant transport of ozone have highlighted, that plant stomatal ozone uptake declines with increasing soil water deficit, because drought prompts stomatal closure (Panek and Goldstein, 2001; Simpson et al., 2003; Nunn et al., 2005). We hypothesize, that stomatal uptake of Hg(0) is impacted by soil conditions of low plant available water in a similar way to ozone. In the future, in-situ soil matrix potential measurements should be used to better quantify the response rate of foliar Hg(0) uptake to soil water content in order to overcome the limitations of the coarse satellite-derived soil water measurements used here. We also suggest determining the possible influence of additional parameters like gravel content and density of soils, rooting depth of trees and atmospheric Hg(0), which could vary within the range of latitude (41° - 55°) of examined forest plots.

3.7 Foliar Hg uptake and geographic and tree-specific parameters

445 We performed linear regressions of average daily foliar Hg uptake rates per forest plot and tree species group (beech, oak, pine, spruce) versus geographic and tree-specific parameters. These parameters include altitude, latitude, average age of trees on plot, average tree diameter at breast height, average daily GLEAM transpiration values and average ERA5-Land 2 m air temperature over the course of the respective sample life periods (see Sect. 2.1). None of the resulting 54 linear regression coefficients were significant given a Bonferroni adjusted p-value = 0.000925. The differences between 2015 and 2017 species-

450 specific averages of daily foliar Hg uptake rates from forest plots, at which foliage sampling took place during both sampling years, were small compared to the standard deviation of daily foliar Hg uptake rates within each sampling year and species (see Table S5 for average and standard deviation values). From the sampling year 2015 to the sampling year 2017 this difference was 0.04 ng Hg $g^{-1}_{d.w.}$ d^{-1} for beech, 2×10^{-4} ng Hg $g^{-1}_{d.w.}$ d^{-1} for oak, 8×10^{-5} ng Hg $g^{-1}_{d.w.}$ d^{-1} for pine (current-season needles) and -3×10^{-3} ng Hg $g^{-1}_{d.w.}$ d^{-1} for spruce (current-season needles). We therefore suggest that differences in daily foliar

455 Hg uptake rates between the sampling years 2015 and 2017 are negligible. In agreement with previous studies (Ollerova et al., 2010; Hutnik et al., 2014; Navrátil et al., 2019; Wohlgemuth et al., 2020; Pleijel et al., 2021), we found a trend of Hg concentrations in differently aged spruce needles with older needles exhibiting higher Hg concentrations (Fig. 7), demonstrating that Hg accumulation continues in older needles. Annual Hg net accumulation seems to slow down in older spruce needles of age classes $y_3 - y_6$ in contrast to needles of age classes $y_0 - y_2$ (Fig. 7), albeit ranges of average Hg

460 concentrations ± standard deviation overlap among older and younger spruce needles, which might be the result of relatively low sample numbers of older needles compared to younger needles (e.g. 3 samples for y_6 vs. 301 samples for y_1). A decline in foliar Hg uptake by older needles could be caused by lower physiological activity, cuticular wax degradation or an increase in Hg re-emission with needle age (Wohlgemuth et al., 2020).
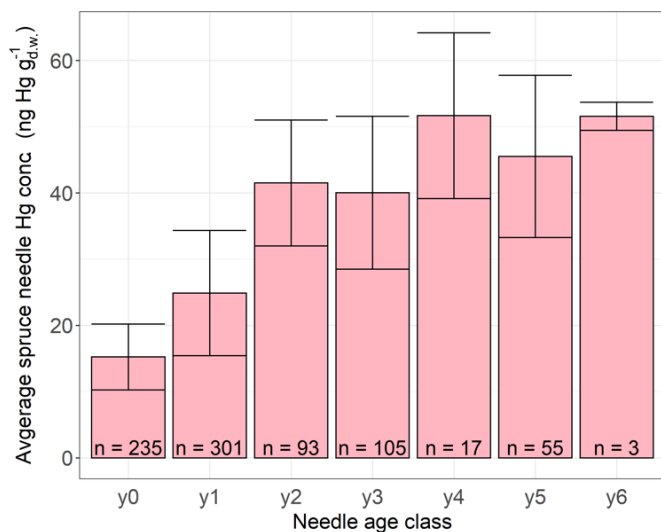
Figure 7. Average Hg concentrations (ng Hg $g_{d.w.}^{-1}$) in spruce needle samples of different ages. Needle age class y_0 corresponds to current-season needles flushed in the year of sampling, y_1 corresponds to one-year old needles, y_2 corresponds to two-year old needles etc. Error bars denote ± one standard deviation between multiple samples, n indicates number of samples.

3.8 Implications for Hg cycle modelling

Our findings suggest, that VPD impacts stomatal Hg(0) uptake by isohydric tree species due to stomatal closure during conditions of high VPD (Fig. 5). Similarly, elongated time periods of low soil water content within the growing season possibly result in a decrease of stomatal conductance to Hg(0) and thus in less foliar Hg(0) uptake by tree species such as beech and pine (Fig. 6). Other meteorological parameters such as temperature may also have an effect on stomatal closure and consequently stomatal Hg(0) uptake (Sect. 3.7). We therefore propose, to refine existing stomatal uptake models for the purpose of exploring the stomatal uptake flux of Hg(0) for common vegetation types across different global regions over the course of the growing season. For this, the sensitivity of species-specific foliar Hg uptake normalized to air Hg(0) concentrations have to be determined in laboratory experiments with regards to elevated VPD, low soil water content or temperature. Eventually, the effect of tree species, VPD, soil water and point in time within the growing season could be implemented in a stomatal Hg deposition model. We propose, that the stomatal flux module of the DO3SE (Deposition of Ozone for Stomatal Exchange) model could serve as a prototype for a stomatal Hg deposition model, because DO3SE provides estimates of stomatal ozone deposition based on plant phenological and meteorological conditions (Emberson et al., 2000, 2018). Projections from stomatal Hg models are particularly relevant for the evaluation of future global environmental Hg cycling, as the stomatal Hg(0) uptake flux exceeds direct Hg(II) wet deposition (Wohlgemuth et al., 2020; Obrist et al., 2021), and quantitatively represents the most relevant deposition pathways to land surfaces, driving the seasonality of Hg(0) in the atmosphere (Obrist, 2007; Jiskra et al., 2018). VPD is projected to increase with rising temperatures under global warming (Yuan et al., 2019; Grossiord et al., 2020), potentially causing a decrease in stomatal foliar Hg(0) uptake fluxes. A diminished

global stomatal foliar Hg(0) uptake flux would result in higher Hg(0) concentrations in the atmosphere and higher Hg deposition fluxes to the ocean (Zhou et al., 2021).

4 Conclusion

490   We created a large European forest dataset for investigating the control of tree physiology and climatic conditions on foliar stomatal Hg(0) uptake. We observed, that foliar Hg concentrations were highly correlated with foliage sampling date (Fig. 2), confirming the notion, that foliage takes up Hg(0) over the entire growing season and over multiple growing seasons in the case of coniferous needles (Fig. 7). Consequently, it is necessary to calculate foliar Hg uptake rates by normalizing foliar Hg concentrations by the time period of Hg(0) accumulation to make foliar Hg values from different sites comparable. For reasons of comparability, foliar Hg uptake rates should ideally be normalized to ambient air Hg(0) concentrations when large variation

495   in atmospheric Hg(0) is expected (e.g. between northern and southern hemispheres, in polluted regions or over long timescales). We found notable differences of daily foliar Hg uptake rates between tree functional groups (broadleaves versus coniferous needles), i.e. Hg uptake rates of broadleaves were higher compared to coniferous needles of the same age by a factor of 3.2 (Fig. 3). Across tree species and within beech and fir, the linear regression coefficients of daily foliar Hg uptake rates versus foliar N concentration were significant (Sect. 3.3). Tree species groups with foliage of lower LMA exhibited

500   higher daily rates of Hg uptake per dry weight of foliage (Sect. 3.4). We set these results within the context of stomatal foliar uptake of atmospheric Hg(0): Deciduous tree species like beech and oak, which exhibit functional traits of high physiological activity (photosynthesis, transpiration) over the time span of one growing season, as represented by high foliar N concentration and low LMA, retain a higher stomatal conductance for diffusive gas exchange. Thus, beech and oak leaves accumulate more Hg per unit dry weight over the same time span relative to needles of coniferous tree species. In addition to tree species-specific

505   metabolism, climatic conditions like current VPD or soil water content, which impacts stomatal gas exchange, can affect foliar Hg uptake. For current-season pine needles, we found a significant negative linear regression coefficient of daily Hg uptake rates versus the average daily proportion of hours within sample life period, during which atmospheric evaporative forcing was high (VPD > 1.2 kPa) (Fig. 5), suggesting, that a reduction of stomatal conductance during conditions of high VPD suppresses foliar Hg(0) uptake. In a similar line of argument, low surface soil water content lowers stomatal conductance and

510   consequently foliar stomatal Hg(0) uptake (Fig. 6). We therefore suggest, that foliar Hg measurements bear the potential to serve as a proxy for stomatal conductance, providing a time-integrated measure for stomatal aperture when taking into account the spatial and temporal variation in atmospheric Hg(0). We call for the implementation of a stomatal Hg(0) deposition model, that takes tree physiology and environmental conditions like VPD or soil water content into account, in order to make projections about this important Hg deposition flux under climate change. The diminution of the vegetation mercury pump in

515   response to drought stress as a result of climate change could result in elevated Hg concentration in the ocean and potentially in marine fish in future, a potential risk which warrants further quantitative studies.

Acknowledgment. We thank Fabienne Bracher and Judith Kobler Waldis for assistance in foliage sample analysis. The evaluation was based on data that was collected by partners of the official UNECE ICP Forests Network (http://icp-forests.net/contributors). We are grateful to all ICP Forests participants who supported the project through foliage sampling, nutrient analysis and cooperation in the logistics of this project. In this context, we particularly thank Martin Maier, Andrea Hölscher and their team from the Department of Soil and Environment at FVA Baden-Württemberg; Daniel Žlindra from the Slovenian Forestry Institute; Nils König from Northwest German Forest Research Institute (NW-FVA); Hans-Peter Dietrich and Stephan Raspe from the Bavarian State Institute of Forestry (LWF Bayern); Michael Tatzber from the Austrian Research Centre for Forests (BFW); Arne Verstraeten and Luc De Geest from the Belgian Research Institute for Nature and Forest (INBO); Sébastien Macé from the French National Forest Office (ONF) and Panagiotis Michopoulos from the Forest Research Institute of Athens (FRIA). We are grateful to Samantha Wittke and Christian Körner for their helpful advice and support on leaf area indices and plant phenology. Special thanks go to Till Kirchner and Anne-Katrin Prescher from Thünen Institute for their assistance in accessing the ICP Forests Database.

Data availability. Foliar Hg concentrations, foliar Hg uptake rates and Hg related metadata are available for download at https://doi.org/10.5281/zenodo.5495179. Please note that coordinates (latitude, longitude) were round to minutes. R-scripts for data analysis and plots of this paper can be found at https://github.com/wohle/Hg_Forests.

ICP Forests proprietory data (N concentrations and forest plot attributes) fall under the publication policy of ICP Forests (Annex II of (Seidling et al., 2017)) and can be accessed from the ICP Forests Database (http://icp-forests.net/page/data-requests) upon request from the Programme Co-ordinating Center (PCC) in Eberswalde, Germany. Foliar Hg concentration values from the Austrian Bio-Indicator Grid can be obtained from BFW upon request (https://bfw.ac.at/rz/bfwcms.web?dok=3687). ERA5-Land data (Muñoz Sabater, 2019) was downloaded from the Copernicus Climate Change Service (C3S) Climate Data Store (https://cds.climate.copernicus.eu/#!/home). Data for the beginning of the growing season of coniferous trees in 2015 and 2017 were provided by members of the PEP725 project (http://www.pep725.eu/). PROBA-V leaf area index values of 300 m resolution and GLEAM transpiration values from 2015 and 2017 were obtained from the VITO Product Distribution Portal (https://land.copernicus.eu/global/products/lai) and the GLEAM server (https://www.gleam.eu/) respectively.

Financial support. This research was funded by the Swiss National Science Foundation (SNSF), project number 174101. The participating countries from the UNECE ICP Forests Network funded the sampling using national funding; among funding agencies are the Natural Resources Institute Finland (Luke), Swiss Federal Institute for Forest, Snow and Landscape Research (WSL), Norwegian Institute of Bioeconomy Research (NIBIO), Norwegian Ministry of Agriculture and Food (LMD), Polish Forest Research Institute (IBL), Polish Ministry of Environment (grants No. 650412-650415), Northwest German Forest Research Institute (NW-FVA), French National Forest Office (ONF), French Ministry of Agriculture, French Agency for

Environment and Energy (ADEME), Slovenian Ministry of Agriculture, Forestry and Food (Public Forest Service, Assignment 1.3), National Institute for Research and Development in Forestry "Marin Dracea" Romania (INCDS). Part of the data was co-financed by the European Commission. The Austrian Bio-Indicator Grid is operated by BFW with funding from the Austrian Ministry of Agriculture, Regions and Tourism.

Author contributions. LW managed the project, coordinated foliar Hg measurements, assembled the Hg dataset, performed the data analysis and wrote the manuscript. PR, BA, AR, LV, PW, VT, NE, MG, PR, AT, MN, AK, MI, PM, SB, DZ, CI supplied foliage samples and metadata and gave scientific input to the manuscript. AF contributed foliar Hg concentrations from the Austrian Bio-Indicator Grid and gave scientific input to the manuscript. GH and CA provided valuable scientific support. MJ designed and set up the SNF project (174101), provided valuable scientific support and contributed to manuscript writing.

Competing interests. The authors declare that they have no conflict of interest.

References

Adams, M. B., Campbell, R. G., Allen, H. L., and Davey, C. B.: Root and foliar nutrient concentrations in loblolly pine: effects of season, site, and fertilization, Forest Sci., 33, 984–996, https://doi.org/10.1093/forestscience/33.4.984, 1987.

AMAP and UNEP: Technical background report to the global mercury assessment 2018. Arctic Monitoring and Assessment Programme, Oslo, Norway/UN Environment Programme, Chemicals and Health Branch, Geneva, Switzerland., https://www.amap.no/documents/doc/technical-background-report-for-the-global-mercury-assessment-2018/1815, 2019.

Austrian Bio-Indicator Grid: https://bfw.ac.at/rz/bfwcms2.web?dok=3687.

Bishop, K., Shanley, J. B., Riscassi, A., de Wit, H. A., Eklöf, K., Meng, B., Mitchell, C., Osterwalder, S., Schuster, P. F., Webster, J., and Zhu, W.: Recent advances in understanding and measurement of mercury in the environment: Terrestrial Hg cycling, Sci. Total Environ., 721, 137647, https://doi.org/10.1016/j.scitotenv.2020.137647, 2020.

Blackwell, B. D. and Driscoll, C. T.: Deposition of mercury in forests along a montane elevation gradient, Environ. Sci. Technol., 49, 5363–5370, https://doi.org/10.1021/es505928w, 2015.

Blackwell, B. D., Driscoll, C. T., Maxwell, J. A., and Holsen, T. M.: Changing climate alters inputs and pathways of mercury deposition to forested ecosystems, Biogeochemistry, 119, 215–228, https://doi.org/10.1007/s10533-014-9961-6, 2014.

Bolton, J. K. and Brown, R. H.: Photosynthesis of grass species differing in carbon dioxide fixation pathways: V. Response of Panicum maximum, Panicum milioides, and tall fescue (Festuca arundinacea) to nitrogen nutrition, Plant Physiol., 66, 97–100, https://doi.org/10.1104/pp.66.1.97, 1980.

Bórnez, K., Descals, A., Verger, A., and Peñuelas, J.: Land surface phenology from VEGETATION and PROBA-V data. Assessment over deciduous forests, Int. J. Appl. Earth Obs., 84, 101974, https://doi.org/10.1016/j.jag.2019.101974, 2020.

Büker, P., Morrissey, T., Briolat, A., Falk, R., Simpson, D., Tuovinen, J.-P., Alonso, R., Barth, S., Baumgarten, M., Grulke, N., Karlsson, P. E., King, J., Lagergren, F., Matyssek, R., Nunn, A., Ogaya, R., Peñuelas, J., Rhea, L., Schaub, M., Uddling, J., Werner, W., and Emberson, L. D.: DO3SE modelling of soil moisture to determine ozone flux to forest trees, Atmos. Chem. Phys., 12, 5537–5562, https://doi.org/10.5194/acp-12-5537-2012, 2012.

Bushey, J. T., Nallana, A. G., Montesdeoca, M. R., and Driscoll, C. T.: Mercury dynamics of a northern hardwood canopy, Atmos. Environ., 42, 6905–6914, https://doi.org/10.1016/j.atmosenv.2008.05.043, 2008.

Cárcer, P. S. de, Vitasse, Y., Peñuelas, J., Jassey, V. E. J., Buttler, A., and Signarbieux, C.: Vapor–pressure deficit and extreme climatic variables limit tree growth, Glob. Change Biol., 24, 1108–1122, https://doi.org/10.1111/gcb.13973, 2018.

Carnicer, J., Barbeta, A., Sperlich, D., Coll, M., and Penuelas, J.: Contrasting trait syndromes in angiosperms and conifers are associated with different responses of tree growth to temperature on a large scale, Front. Plant Sci., 4, https://doi.org/10.3389/fpls.2013.00409, 2013.

CLRTAP: Revised Chapter 3 of the Manual on Methodologies and Criteria for Modelling and Mapping Critical Loads and Levels and Air Pollution Effects, Risks and Trends: Mapping Critical Levels for Vegetation., https://www.umweltbundesamt.de/en/manual-for-modelling-mapping-critical-loads-levels, 2017.

Coll, M., Peñuelas, J., Ninyerola, M., Pons, X., and Carnicer, J.: Multivariate effect gradients driving forest demographic responses in the Iberian Peninsula, Forest Ecol. Manag., 303, 195–209, https://doi.org/10.1016/j.foreco.2013.04.010, 2013.

Cools, N. and De Vos, B.: Part X: Sampling and analysis of soil. In: UNECE ICP Forests, Programme Coordinating Centre (ed.): Manual on methods and criteria for harmonized sampling, assessment, monitoring and analysis of the effects of air pollution on forests., Thünen Institute of Forest Ecosystems, Eberswalde, Germany, http://icp-forests.net/page/icp-forests-manual, 2020.

Demers, J. D., Blum, J. D., and Zak, D. R.: Mercury isotopes in a forested ecosystem: Implications for air-surface exchange dynamics and the global mercury cycle, Global Biochem. Cy., 27, 222–238, https://doi.org/10.1002/gbc.20021, 2013.

Dierckx, W., Sterckx, S., Benhadj, I., Livens, S., Duhoux, G., Van Achteren, T., Francois, M., Mellab, K., and Saint, G.: PROBA-V mission for global vegetation monitoring: standard products and image quality, Int. J. Remote Sens., 35, 2589–2614, https://doi.org/10.1080/01431161.2014.883097, 2014.

Dobbertin, M. and Neumann, M.: Part V: Tree Growth. In: UNECE ICP Forests, Programme Coordinating Centre (ed.): Manual on methods and criteria for harmonized sampling, assessment, monitoring and analysis of the effects of air pollution on forests., Thünen Institute of Forest Ecosystems, Eberswalde, Germany, http://icp-forests.net/page/icp-forests-manual, 2016.

Domec, J.-C., Noormets, A., King, J. S., Sun, G., Mcnulty, S. G., Gavazzi, M. J., Boggs, J. L., and Treasure, E. A.: Decoupling the influence of leaf and root hydraulic conductances on stomatal conductance and its sensitivity to vapour pressure deficit as

soil dries in a drained loblolly pine plantation, Plant Cell Environ., 32, 980–991, https://doi.org/10.1111/j.1365-3040.2009.01981.x, 2009.

625 Drenner, R. W., Chumchal, M. M., Jones, C. M., Lehmann, C. M. B., Gay, D. A., and Donato, D. I.: Effects of mercury deposition and coniferous forests on the mercury contamination of fish in the South Central United States, Environ. Sci. Technol., 47, 1274–1279, https://doi.org/10.1021/es303734n, 2013.

Driscoll, C. T., Mason, R. P., Chan, H. M., Jacob, D. J., and Pirrone, N.: Mercury as a global pollutant: sources, pathways, and effects, Environ. Sci. Technol., 47, 4967–4983, https://doi.org/10.1021/es305071v, 2013.

630 Ellsworth, D. S. and Reich, P. B.: Canopy structure and vertical patterns of photosynthesis and related leaf traits in a deciduous forest, Oecologia, 96, 169–178, https://doi.org/10.1007/BF00317729, 1993.

Emberson, L. D., Ashmore, M. R., Cambridge, H. M., and Simpson, D.: Modelling stomatal ozone flux across Europe, Environ. Pollut., 11, 2000.

Emberson, L. D., Pleijel, H., Ainsworth, E. A., van den Berg, M., Ren, W., Osborne, S., Mills, G., Pandey, D., Dentener, F.,
635 Büker, P., Ewert, F., Koeble, R., and Van Dingenen, R.: Ozone effects on crops and consideration in crop models, Eur. J. Agron., 100, 19–34, https://doi.org/10.1016/j.eja.2018.06.002, 2018.

EMEP: Present state of Hg(0) data, http://ebas-data.nilu.no/default.aspx, 2021.

Enrico, M., Roux, G. L., Marusczak, N., Heimbürger, L.-E., Claustres, A., Fu, X., Sun, R., and Sonke, J. E.: Atmospheric mercury transfer to peat bogs dominated by gaseous elemental mercury dry deposition, Environ. Sci. Technol., 50, 2405–2412,
640 https://doi.org/10.1021/acs.est.5b06058, 2016.

EU: European Commission, 2011/833/EU: Commission Decision of 12 December 2011 on the reuse of Commission documents, 2011.

Evans, J. R.: Photosynthesis and nitrogen relationships in leaves of C3 plants, Oecologia, 78, 9–19, https://doi.org/10.1007/BF00377192, 1989.

645 Evans, J. R. and Poorter, H.: Photosynthetic acclimation of plants to growth irradiance: the relative importance of specific leaf area and nitrogen partitioning in maximizing carbon gain, Plant Cell Environ., 24, 755–767, https://doi.org/10.1046/j.1365-3040.2001.00724.x, 2001.

Fleck, S., Cools, N., De Vos, B., Meesenburg, H., and Fischer, R.: The Level II aggregated forest soil condition database links soil physicochemical and hydraulic properties with long-term observations of forest condition in Europe, Ann. For. Sci., 73,
650 945–957, https://doi.org/10.1007/s13595-016-0571-4, 2016.

Franks, P. J. and Farquhar, G. D.: A relationship between humidity response, growth form and photosynthetic operating point in C3 plants, Plant Cell Environ., 22, 1337–1349, https://doi.org/10.1046/j.1365-3040.1999.00494.x, 1999.

Fuster, B., Sánchez-Zapero, J., Camacho, F., García-Santos, V., Verger, A., Lacaze, R., Weiss, M., Baret, F., and Smets, B.: Quality assessment of PROBA-V LAI, fAPAR and fCOVER collection 300 m products of Copernicus Global Land Service,
655 Remote Sens., 12, 1017, https://doi.org/10.3390/rs12061017, 2020.

Graydon, J. A., St. Louis, V. L., Hintelmann, H., Lindberg, S. E., Sandilands, K. A., Rudd, J. W. M., Kelly, C. A., Hall, B. D., and Mowat, L. D.: Long-term wet and dry deposition of total and methyl mercury in the remote boreal ecoregion of Canada, Environ. Sci. Technol., 42, 8345–8351, https://doi.org/10.1021/es801056j, 2008.

Grigal, D. F.: Mercury sequestration in forests and peatlands, J. Environ. Qual., 32, 393, https://doi.org/10.2134/jeq2003.3930, 2003.

Grossiord, C., Buckley, T. N., Cernusak, L. A., Novick, K. A., Poulter, B., Siegwolf, R. T. W., Sperry, J. S., and McDowell, N. G.: Plant responses to rising vapor pressure deficit, New Phytol., 226, 1550–1566, https://doi.org/10.1111/nph.16485, 2020.

Grünhage, L., Braden, H., Bender, J., Burkart, S., Lehmann, Y., and Schröder, M.: Evaluation of the ozone-related risk for winter wheat at local scale with the CRO3PS model, Gefahrstoffe - Reinhaltung der Luft, 71, 9, https://www.researchgate.net/publication/278672267_Evaluation_of_the_ozone-related_risk_for_winter_wheat_at_local_scale_with_the_CRO3PS_model, 2011.

Grünhage, L., Pleijel, H., Mills, G., Bender, J., Danielsson, H., Lehmann, Y., Castell, J.-F., and Bethenod, O.: Updated stomatal flux and flux-effect models for wheat for quantifying effects of ozone on grain yield, grain mass and protein yield, Environ. Pollut., 165, 147–157, https://doi.org/10.1016/j.envpol.2012.02.026, 2012.

Hatcher, P. E.: Seasonal and age-related variation in the needle quality of five conifer species, Oecologia, 85, 200–212, https://doi.org/10.1007/BF00319402, 1990.

Hikosaka, K.: Interspecific difference in the photosynthesis–nitrogen relationship: patterns, physiological causes, and ecological importance, J. Plant. Res., 117, 481–494, https://doi.org/10.1007/s10265-004-0174-2, 2004.

Huber, W., Carey, V. J., Gentleman, R., Anders, S., Carlson, M., Carvalho, B. S., Bravo, H. C., Davis, S., Gatto, L., Girke, T., Gottardo, R., Hahne, F., Hansen, K. D., Irizarry, R. A., Lawrence, M., Love, M. I., MacDonald, J., Obenchain, V., Oleś, A. K., Pagès, H., Reyes, A., Shannon, P., Smyth, G. K., Tenenbaum, D., Waldron, L., and Morgan, M.: Orchestrating high-throughput genomic analysis with Bioconductor, Nat. Methods, 12, 115–121, https://doi.org/10.1038/nmeth.3252, 2015.

Hutnik, R. J., McClenahen, J. R., Long, R. P., and Davis, D. D.: Mercury accumulation in Pinus nigra (Austrian Pine), Northeast. Nat., 21, 529–540, https://doi.org/10.1656/045.021.0402, 2014.

Iglewicz, B. and Hoaglin, D. C.: How to detect and handle outliers, ASQC Quality Press, Milwaukee, Wis, 87 pp., 1993.

Iverfeldt, Å.: Mercury in forest canopy throughfall water and its relation to atmospheric deposition, Water Air Soil Poll., 56, 553–564, https://doi.org/10.1007/BF00342299, 1991.

Jiskra, M., Wiederhold, J. G., Skyllberg, U., Kronberg, R.-M., Hajdas, I., and Kretzschmar, R.: Mercury deposition and re-emission pathways in boreal forest soils investigated with Hg isotope signatures, Environ. Sci. Technol., 49, 7188–7196, 2015.

Jiskra, M., Wiederhold, J. G., Skyllberg, U., Kronberg, R.-M., and Kretzschmar, R.: Source tracing of natural organic matter bound mercury in boreal forest runoff with mercury stable isotopes, Environ. Sci.: Processes Impacts, 19, 1235–1248, https://doi.org/10.1039/C7EM00245A, 2017.

Jiskra, M., Sonke, J. E., Obrist, D., Bieser, J., Ebinghaus, R., Myhre, C. L., Pfaffhuber, K. A., Wängberg, I., Kyllönen, K., Worthy, D., Martin, L. G., Labuschagne, C., Mkololo, T., Ramonet, M., Magand, O., and Dommergue, A.: A vegetation control on seasonal variations in global atmospheric mercury concentrations, Nat. Geosci., 1–7, https://doi.org/10.1038/s41561-018-0078-8, 2018.

Jiskra, M., Sonke, J. E., Agnan, Y., Helmig, D., and Obrist, D.: Insights from mercury stable isotopes on terrestrial–atmosphere exchange of Hg(0) in the Arctic tundra, Biogeosciences, 16, 4051–4064, https://doi.org/10.5194/bg-16-4051-2019, 2019.

Jonard, M., Fürst, A., Verstraeten, A., Thimonier, A., Timmermann, V., Potočić, N., Waldner, P., Benham, S., Hansen, K.,
695   Merilä, P., Ponette, Q., Cruz, A. C. de la, Roskams, P., Nicolas, M., Croisé, L., Ingerslev, M., Matteucci, G., Decinti, B.,
Bascietto, M., and Rautio, P.: Tree mineral nutrition is deteriorating in Europe, Glob. Change Biol., 21, 418–430,
https://doi.org/10.1111/gcb.12657, 2015.

Körner, C.: Plant–Environment Interactions, in: Strasburger's Plant Sciences: Including Prokaryotes and Fungi, edited by:
Bresinsky, A., Körner, C., Kadereit, J. W., Neuhaus, G., and Sonnewald, U., Springer, Berlin, Heidelberg, 1065–1166,
700   https://doi.org/10.1007/978-3-642-15518-5_12, 2013.

Körner,   C.:   Concepts   in   empirical   plant   ecology,   Plant   Ecol.   Divers.,   11,   405–428,
https://doi.org/10.1080/17550874.2018.1540021, 2018.

Körner, Ch., Scheel, J., and Bauer, H.: Maximum leaf diffusive conductance in vascular plants, Photosynthetica, 13, 45–82,
1979.

705   Laacouri, A., Nater, E. A., and Kolka, R. K.: Distribution and uptake dynamics of mercury in leaves of common deciduous
tree species in Minnesota, U.S.A., Environ. Sci. Technol., 47, 10462–10470, https://doi.org/10.1021/es401357z, 2013.

Lagergren, F. and Lindroth, A.: Transpiration response to soil moisture in pine and spruce trees in Sweden, Agr. Forest
Meteorol., 112, 67–85, https://doi.org/10.1016/S0168-1923(02)00060-6, 2002.

Lin, Y.-S., Medlyn, B. E., Duursma, R. A., Prentice, I. C., Wang, H., Baig, S., Eamus, D., de Dios, V. R., Mitchell, P.,
710   Ellsworth, D. S., de Beeck, M. O., Wallin, G., Uddling, J., Tarvainen, L., Linderson, M.-L., Cernusak, L. A., Nippert, J. B.,
Ocheltree, T. W., Tissue, D. T., Martin-StPaul, N. K., Rogers, A., Warren, J. M., De Angelis, P., Hikosaka, K., Han, Q., Onoda,
Y., Gimeno, T. E., Barton, C. V. M., Bennie, J., Bonal, D., Bosc, A., Löw, M., Macinins-Ng, C., Rey, A., Rowland, L.,
Setterfield, S. A., Tausz-Posch, S., Zaragoza-Castells, J., Broadmeadow, M. S. J., Drake, J. E., Freeman, M., Ghannoum, O.,
Hutley, L. B., Kelly, J. W., Kikuzawa, K., Kolari, P., Koyama, K., Limousin, J.-M., Meir, P., Lola da Costa, A. C., Mikkelsen,
715   T. N., Salinas, N., Sun, W., and Wingate, L.: Optimal stomatal behaviour around the world, Nat. Clim. Chang., 5, 459–464,
https://doi.org/10.1038/nclimate2550, 2015.

Lodenius, M., Tulisalo, E., and Soltanpour-Gargari, A.: Exchange of mercury between atmosphere and vegetation under
contaminated conditions, Sci. Total Environ., 304, 169–174, https://doi.org/10.1016/S0048-9697(02)00566-1, 2003.

Loomis, R. S.: On the utility of nitrogen in leaves, PNAS, 94, 13378–13379, https://doi.org/10.1073/pnas.94.25.13378, 1997.

720   Manceau, A., Wang, J., Rovezzi, M., Glatzel, P., and Feng, X.: Biogenesis of mercury–sulfur nanoparticles in plant leaves
from atmospheric gaseous mercury, Environ. Sci. Technol., 52, 3935–3948, https://doi.org/10.1021/acs.est.7b05452, 2018.

Martens, B., Miralles, D. G., Lievens, H., Schalie, R. van der, Jeu, R. A. M. de, Fernández-Prieto, D., Beck, H. E., Dorigo, W.
A., and Verhoest, N. E. C.: GLEAM v3: satellite-based land evaporation and root-zone soil moisture, Geosci. Model Dev., 10,
1903–1925, https://doi.org/10.5194/gmd-10-1903-2017, 2017.

725   Martínez-Ferri, E., Balaguer, L., Valladares, F., Chico, J. M., and Manrique, E.: Energy dissipation in drought-avoiding and
drought-tolerant tree species at midday during the Mediterranean summer, Tree Physiol., 20, 131–138,
https://doi.org/10.1093/treephys/20.2.131, 2000.

McAdam, S. A. M. and Brodribb, T. J.: The evolution of mechanisms driving the stomatal response to vapor pressure deficit,
Plant Physiol., 167, 833–843, https://doi.org/10.1104/pp.114.252940, 2015.

730 Mediavilla, S. and Escudero, A.: Relative growth rate of leaf biomass and leaf nitrogen content in several mediterranean woody species, Plant Ecol., 168, 321–332, https://doi.org/10.1023/A:1024496717918, 2003.

Mellander, P.-E., Bishop, K., and Lundmark, T.: The influence of soil temperature on transpiration: a plot scale manipulation in a young Scots pine stand, Forest Ecol. Manag., 195, 15–28, https://doi.org/10.1016/j.foreco.2004.02.051, 2004.

Meziane, D. and Shipley, B.: Direct and indirect relationships between specific leaf area, leaf nitrogen and leaf gas exchange.
735 Effects of irradiance and nutrient supply, Ann. Bot., 88, 915–927, https://doi.org/10.1006/anbo.2001.1536, 2001.

Miralles, D. G., Holmes, T. R. H., De Jeu, R. A. M., Gash, J. H., Meesters, A. G. C. A., and Dolman, A. J.: Global land-surface evaporation estimated from satellite-based observations, Hydrol. Earth Syst. Sc., 15, 453–469, https://doi.org/10.5194/hess-15-453-2011, 2011.

Muñoz Sabater, J.: ERA5-Land hourly data from 1981 to present. Copernicus Climate Change Service (C3S) Climate Data
740 Store (CDS), https://cds.climate.copernicus.eu/cdsapp#!/dataset/reanalysis-era5-land?tab=overview, 2019.

Navrátil, T., Shanley, J. B., Rohovec, J., Oulehle, F., Šimeček, M., Houška, J., and Cudlín, P.: Soil mercury distribution in adjacent coniferous and deciduous stands highly impacted by acid rain in the Ore Mountains, Czech Republic, Appl. Geochem., 75, 63–75, https://doi.org/10.1016/j.apgeochem.2016.10.005, 2016.

Navrátil, T., Nováková, T., Roll, M., Shanley, J. B., Kopáček, J., Rohovec, J., Kaňa, J., and Cudlín, P.: Decreasing litterfall
745 mercury deposition in central European coniferous forests and effects of bark beetle infestation, Sci. Total Environ., 682, 213–225, https://doi.org/10.1016/j.scitotenv.2019.05.093, 2019.

Niinemets, Ü. and Tenhunen, J. D.: A model separating leaf structural and physiological effects on carbon gain along light gradients for the shade-tolerant species Acer saccharum, Plant Cell Environ., 20, 845–866, https://doi.org/10.1046/j.1365-3040.1997.d01-133.x, 1997.

750 Nunn, A. J., Kozovits, A. R., Reiter, I. M., Heerdt, C., Leuchner, M., Lütz, C., Liu, X., Lo¨w, M., Winkler, J. B., Grams, T. E. E., Häberle, K.-H., Werner, H., Fabian, P., Rennenberg, H., and Matyssek, R.: Comparison of ozone uptake and sensitivity between a phytotron study with young beech and a field experiment with adult beech (Fagus sylvatica), Environ. Pollut., 137, 494–506, https://doi.org/10.1016/j.envpol.2005.01.036, 2005.

Obrist, D.: Atmospheric mercury pollution due to losses of terrestrial carbon pools?, Biogeochemistry, 85, 119–123,
755 https://doi.org/10.1007/s10533-007-9108-0, 2007.

Obrist, D., Roy, E. M., Harrison, J. L., Kwong, C. F., Munger, J. W., Moosmüller, H., Romero, C. D., Sun, S., Zhou, J., and Commane, R.: Previously unaccounted atmospheric mercury deposition in a midlatitude deciduous forest, PNAS, 118, https://doi.org/10.1073/pnas.2105477118, 2021.

Ollerova, H., Maruskova, A., Kontrisova, O., and Pliestikova, L.: Mercury accumulation in Picea abies (L.) Karst. needles
760 with regard to needle age, Pol. J. Environ. Stud., 19, 1401–1404, 2010.

Panek, J. A. and Goldstein, A. H.: Response of stomatal conductance to drought in ponderosa pine: implications for carbon and ozone uptake, Tree Physiol., 21, 337–344, https://doi.org/10.1093/treephys/21.5.337, 2001.

Pleijel, H., Klingberg, J., Nerentorp, M., Broberg, M. C., Nyirambangutse, B., Munthe, J., and Wallin, G.: Mercury accumulation in leaves of different plant types - the significance of tissue age and specific leaf area, Biogeosciences, 18, 6313-
765 6328, https://doi.org/10.5194/bg-18-6313-2021, 2021.

Raspe, S., Bastrup-Birk, A., Fleck, S., Weis, W., Mayer, H., Meesenburg, H., Wagner, M., Schindler, D., and Gartner, K.: Chapter 17 - Meteorology, in: Developments in Environmental Science, vol. 12, edited by: Ferretti, M. and Fischer, R., Elsevier, 319–336, https://doi.org/10.1016/B978-0-08-098222-9.00017-0, 2013.

770   Rautio, P., Fürst, A., Stefan, K., Raitio, H., and Bartels, U.: Part XII: Sampling and analysis of needles and leaves. In: UNECE ICP Forests, Programme Coordinating Centre (ed.): Manual on methods and criteria for harmonized sampling, assessment, monitoring and analysis of the effects of air pollution on forests., Thünen Institute of Forest Ecosystems, Eberswalde, Germany, http://icp-forests.net/page/icp-forests-manual, 2016.

Rea, A. W., Keeler, G. J., and Scherbatskoy, T.: The deposition of mercury in throughfall and litterfall in the Lake Champlain Watershed: A short-term study, Atmos. Environ., 30, 3257–3263, https://doi.org/10.1016/1352-2310(96)00087-8, 1996.

775   Rea, A. W., Lindberg, S. E., and Keeler, G. J.: Dry deposition and foliar leaching of mercury and selected trace elements in deciduous forest throughfall, Atmos. Environ., 35, 3453–3462, https://doi.org/10.1016/S1352-2310(01)00133-9, 2001.

Rea, A. W., Lindberg, S. E., Scherbatskoy, T., and Keeler, G. J.: Mercury accumulation in foliage over time in two northern mixed-hardwood forests, Water Air Soil Poll., 133, 49–67, 2002.

Reich, P. B., Walters, M. B., Ellsworth, D. S., Vose, J. M., Volin, J. C., Gresham, C., and Bowman, W. D.: Relationships of
780   leaf dark respiration to leaf nitrogen, specific leaf area and leaf life-span: a test across biomes and functional groups, Oecologia, 114, 471–482, https://doi.org/10.1007/s004420050471, 1998.

Reich, P. B., Ellsworth, D. S., Walters, M. B., Vose, J. M., Gresham, C., Volin, J. C., and Bowman, W. D.: Generality of leaf trait relationships: a test across six biomes, Ecology, 80, 1955–1969, https://doi.org/10.1890/0012-9658(1999)080[1955:GOLTRA]2.0.CO;2, 1999.

785   Reich, P. B., Wright, I. J., Cavender-Bares, J., Craine, J. M., Oleksyn, J., Westoby, M., and Walters, M. B.: The evolution of plant functional variation: traits, spectra, and strategies, Int. J. Plant Sci., 164, S143–S164, https://doi.org/10.1086/374368, 2003.

Risch, M. R., DeWild, J. F., Krabbenhoft, D. P., Kolka, R. K., and Zhang, L.: Litterfall mercury dry deposition in the eastern USA, Environ. Pollut., 161, 284–290, https://doi.org/10.1016/j.envpol.2011.06.005, 2012.

790   Risch, M. R., DeWild, J. F., Gay, D. A., Zhang, L., Boyer, E. W., and Krabbenhoft, D. P.: Atmospheric mercury deposition to forests in the eastern USA, Environ. Pollut., 228, 8–18, https://doi.org/10.1016/j.envpol.2017.05.004, 2017.

Rosati, A., Esparza, G., DeJong, T. M., and Pearcy, R. W.: Influence of canopy light environment and nitrogen availability on leaf photosynthetic characteristics and photosynthetic nitrogen-use efficiency of field-grown nectarine trees, Tree Physiol., 19, 173–180, https://doi.org/10.1093/treephys/19.3.173, 1999.

795   Rötzer, T. and Chmielewski, F.: Phenological maps of Europe, Clim. Res., 18, 249–257, https://doi.org/10.3354/cr018249, 2001.

Running, S. W. and Coughlan, J. C.: A general model of forest ecosystem processes for regional applications I. Hydrologic balance, canopy gas exchange and primary production processes, Ecol. Model, 42, 125–154, https://doi.org/10.1016/0304-3800(88)90112-3, 1988.

800   Rutter, A. P., Schauer, J. J., Shafer, M. M., Creswell, J. E., Olson, M. R., Robinson, M., Collins, R. M., Parman, A. M., Katzman, T. L., and Mallek, J. L.: Dry deposition of gaseous elemental mercury to plants and soils using mercury stable isotopes in a controlled environment, Atmos. Environ., 45, 848–855, https://doi.org/10.1016/j.atmosenv.2010.11.025, 2011.

Saxton, K. E. and Rawls, W. J.: Soil water characteristic estimates by texture and organic matter for hydrologic solutions, Soil Sci. Soc. Am. J., 70, 1569–1578, https://doi.org/10.2136/sssaj2005.0117, 2006.

805 Schulze, E.-D., Kelliher, F. M., Körner, C., Lloyd, J., and Leuning, R.: Relationships among maximum stomatal conductance, ecosystem surface conductance, carbon assimilation rate, and plant nitrogen nutrition: A global ecology scaling exercise, Annu. Rev. Ecol. Sys., 36, 1994.

Schwarz, P. A., Fahey, T. J., and Dawson, T. E.: Seasonal air and soil temperature effects on photosynthesis in red spruce (Picea rubens) saplings, Tree Physiol., 17, 187–194, https://doi.org/10.1093/treephys/17.3.187, 1997.

810 Schwesig, D. and Matzner, E.: Pools and fluxes of mercury and methylmercury in two forested catchments in Germany, Sci. Total Environ., 260, 213–223, https://doi.org/10.1016/S0048-9697(00)00565-9, 2000.

Seidling, W., Hansen, K., Strich, S., and Lorenz, M.: Part I: Objectives, Strategy and Implementation of ICP Forests. In: UNECE ICP Forests, Programme Coordinating Centre (ed.): Manual on methods and criteria for harmonized sampling, assessment, monitoring and analysis of the effects of air pollution on forests., Thünen Institute of Forest Ecosystems,
815 Eberswalde, Germany, http://icp-forests.net/page/icp-forests-manual, 2017.

Simpson, D., Tuovinen, J.-P., Emberson, L., and Ashmore, M. R.: Characteristics of an ozone deposition module II: Sensitivity analysis, Water Air Soil Poll., 143, 123–137, https://doi.org/10.1023/A:1022890603066, 2003.

Sonke, J. E., Teisserenc, R., Heimbürger-Boavida, L.-E., Petrova, M. V., Maruszczak, N., Dantec, T. L., Chupakov, A. V., Li, C., Thackray, C. P., Sunderland, E. M., Tananaev, N., and Pokrovsky, O. S.: Eurasian river spring flood observations support
820 net Arctic Ocean mercury export to the atmosphere and Atlantic Ocean, PNAS, 115, E11586–E11594, https://doi.org/10.1073/pnas.1811957115, 2018.

Sprovieri, F., Pirrone, N., Bencardino, M., D'Amore, F., Angot, H., Barbante, C., Brunke, E.-G., Arcega-Cabrera, F., Cairns, W., Comero, S., Diéguez, M. del C., Dommergue, A., Ebinghaus, R., Feng, X. B., Fu, X., Garcia, P. E., Gawlik, B. M., Hageström, U., Hansson, K., Horvat, M., Kotnik, J., Labuschagne, C., Magand, O., Martin, L., Mashyanov, N., Mkololo,
825 T., Munthe, J., Obolkin, V., Ramirez Islas, M., Sena, F., Somerset, V., Spandow, P., Vardè, M., Walters, C., Wängberg, I., Weigelt, A., Yang, X., and Zhang, H.: Five-year records of mercury wet deposition flux at GMOS sites in the Northern and Southern hemispheres, Atmos. Chem. Phys., 17, 2689–2708, https://doi.org/10.5194/acp-17-2689-2017, 2017.

Teixeira, D. C., Lacerda, L. D., and Silva-Filho, E. V.: Foliar mercury content from tropical trees and its correlation with physiological parameters in situ, Environ. Pollut., 242, 1050–1057, https://doi.org/10.1016/j.envpol.2018.07.120, 2018.

830 Templ, B., Koch, E., Bolmgren, K., Ungersböck, M., Paul, A., Scheifinger, H., Rutishauser, T., Busto, M., Chmielewski, F.-M., Hájková, L., Hodzić, S., Kaspar, F., Pietragalla, B., Romero-Fresneda, R., Tolvanen, A., Vučetič, V., Zimmermann, K., and Zust, A.: Pan European Phenological database (PEP725): a single point of access for European data, Int. J. Biometeorol., 62, 1109–1113, https://doi.org/10.1007/s00484-018-1512-8, 2018.

Tørseth, K., Aas, W., Breivik, K., Fjæraa, A. M., Fiebig, M., Hjellbrekke, A. G., Lund Myhre, C., Solberg, S., and Yttri, K.
835 E.: Introduction to the European Monitoring and Evaluation Programme (EMEP) and observed atmospheric composition change during 1972-2009, Atmos. Chem. Phys., 12, 5447–5481, https://doi.org/10.5194/acp-12-5447-2012, 2012.

Travnikov, O., Angot, H., Artaxo, P., Bencardino, M., Bieser, J., D'Amore, F., Dastoor, A., De Simone, F., Diéguez, M. del C., Dommergue, A., Ebinghaus, R., Feng, X. B., Gencarelli, C. N., Hedgecock, I. M., Magand, O., Martin, L., Matthias, V., Mashyanov, N., Pirrone, N., Ramachandran, R., Read, K. A., Ryjkov, A., Selin, N. E., Sena, F., Song, S., Sprovieri, F., Wip,
840 D., Wängberg, I., and Yang, X.: Multi-model study of mercury dispersion in the atmosphere: atmospheric processes and model evaluation, Atmos. Chem. Phys., 17, 5271–5295, https://doi.org/10.5194/acp-17-5271-2017, 2017.

Tsuji, S., Nakashizuka, T., Kuraji, K., Kume, A., and Hanba, Y. T.: Sensitivity of stomatal conductance to vapor pressure deficit and its dependence on leaf water relations and wood anatomy in nine canopy tree species in a Malaysian wet tropical rainforest, Trees, 34, 1299–1311, https://doi.org/10.1007/s00468-020-01998-5, 2020.

845 UN Environment: Global Mercury Assessment 2018, Chemicals and Health Branch, Geneva, Switzerland, 2019.

Vesterdal, L., Schmidt, I. K., Callesen, I., Nilsson, L. O., and Gundersen, P.: Carbon and nitrogen in forest floor and mineral soil under six common European tree species, Forest Ecol. Manag., 255, 35–48, https://doi.org/10.1016/j.foreco.2007.08.015, 2008.

Vilhar, U., Beuker, E., Mizunuma, T., Skudnik, M., Lebourgeois, F., Soudani, K., and Wilkinson, M.: Chapter 9 - Tree
850 Phenology, in: Developments in Environmental Science, vol. 12, edited by: Ferretti, M. and Fischer, R., Elsevier, 169–182, https://doi.org/10.1016/B978-0-08-098222-9.00009-1, 2013.

Wang, X., Bao, Z., Lin, C.-J., Yuan, W., and Feng, X.: Assessment of global mercury deposition through litterfall, Environ. Sci. Technol., 50, 8548–8557, https://doi.org/10.1021/acs.est.5b06351, 2016.

Wang, X., Yuan, W., Lin, C.-J., Luo, J., Wang, F., Feng, X., Fu, X., and Liu, C.: Underestimated sink of atmospheric mercury
855 in a deglaciated forest chronosequence, Environ. Sci. Technol., 54, 8083–8093, https://doi.org/10.1021/acs.est.0c01667, 2020.

Weiss-Penzias, P. S., Ortiz, C., Acosta, R. P., Heim, W., Ryan, J. P., Fernandez, D., Collett, J. L., and Flegal, A. R.: Total and monomethyl mercury in fog water from the central California coast, Geophys. Res. Lett., 39, https://doi.org/10.1029/2011GL050324, 2012.

Wilson, K. B., Baldocchi, D. D., and Hanson, P. J.: Spatial and seasonal variability of photosynthetic parameters and their
860 relationship to leaf nitrogen in a deciduous forest, Tree Physiol., 20, 565–578, https://doi.org/10.1093/treephys/20.9.565, 2000.

Wohlgemuth, L., Osterwalder, S., Joseph, C., Kahmen, A., Hoch, G., Alewell, C., and Jiskra, M.: A bottom-up quantification of foliar mercury uptake fluxes across Europe, Biogeosciences, 17, 6441–6456, https://doi.org/10.5194/bg-17-6441-2020, 2020.

Wright, I. J., Reich, P. B., Westoby, M., Ackerly, D. D., Baruch, Z., Bongers, F., Cavender-Bares, J., Chapin, T., Cornelissen,
865 J. H. C., Diemer, M., Flexas, J., Garnier, E., Groom, P. K., Gulias, J., Hikosaka, K., Lamont, B. B., Lee, T., Lee, W., Lusk, C., Midgley, J. J., Navas, M.-L., Niinemets, Ü., Oleksyn, J., Osada, N., Poorter, H., Poot, P., Prior, L., Pyankov, V. I., Roumet, C., Thomas, S. C., Tjoelker, M. G., Veneklaas, E. J., and Villar, R.: The worldwide leaf economics spectrum, Nature, 428, 821–827, https://doi.org/10.1038/nature02403, 2004.

Wright, L. P., Zhang, L., and Marsik, F. J.: Overview of mercury dry deposition, litterfall, and throughfall studies, Atmos.
870 Chem. Phys., 16, 13399–13416, 2016.

Yang, Y., Yanai, R. D., Montesdeoca, M., and Driscoll, C. T.: Measuring mercury in wood: challenging but important, Int. J. Environ. An. Ch., 97, 456–467, https://doi.org/10.1080/03067319.2017.1324852, 2017.

Yu, B., Fu, X., Yin, R., Zhang, H., Wang, X., Lin, C.-J., Wu, C., Zhang, Y., He, N., Fu, P., Wang, Z., Shang, L., Sommar, J., Sonke, J. E., Maurice, L., Guinot, B., and Feng, X.: Isotopic composition of atmospheric mercury in china: new evidence for
875 sources and transformation processes in air and in vegetation, Environ. Sci. Technol., 50, 9262–9269, https://doi.org/10.1021/acs.est.6b01782, 2016.

Yuan, W., Zheng, Y., Piao, S., Ciais, P., Lombardozzi, D., Wang, Y., Ryu, Y., Chen, G., Dong, W., Hu, Z., Jain, A. K., Jiang, C., Kato, E., Li, S., Lienert, S., Liu, S., Nabel, J. E. M. S., Qin, Z., Quine, T., Sitch, S., Smith, W. K., Wang, F., Wu, C., Xiao,

Z., and Yang, S.: Increased atmospheric vapor pressure deficit reduces global vegetation growth, Sci. Adv., 5, https://doi.org/10.1126/sciadv.aax1396, 2019.

Zhou, J., Obrist, D., Dastoor, A., Jiskra, M., and Ryjkov, A.: Vegetation uptake of mercury and impacts on global cycling, Nat. Rev. Earth Environ., 1–16, https://doi.org/10.1038/s43017-021-00146-y, 2021.

Zweifel, R., Steppe, K., and Sterck, F. J.: Stomatal regulation by microclimate and tree water relations: interpreting ecophysiological field data with a hydraulic plant model, J. Exp. Bot., 58, 2113–2131, https://doi.org/10.1093/jxb/erm050, 2007.

Zweifel, R., Rigling, A., and Dobbertin, M.: Species-specific stomatal response of trees to drought – a link to vegetation dynamics?, J. Veg. Sci., 20, 442–454, https://doi.org/10.1111/j.1654-1103.2009.05701.x, 2009.

890